

M. BARDAK

IZMIR KATIP CELEBI UNIVERSITY

2019

**IZMIR KATIP CELEBI UNIVERSITY
GRADUATE SCHOOL OF NATURAL AND APPLIED SCIENCES**

**INVESTIGATION OF PULSED ELECTROMAGNETIC FIELD
WITH HIGH RESOLUTION WIRELESS SENSOR NETWORK**



**M.Sc. THESIS
Merve BARDAK**

Department of Biomedical Technologies

JANUARY 2019

**IZMIR KATIP CELEBI UNIVERSITY
GRADUATE SCHOOL OF NATURAL AND APPLIED
SCIENCES**

**INVESTIGATION OF PULSED ELECTROMAGNETIC FIELD
WITH HIGH RESOLUTION WIRELESS SENSOR NETWORK**

M.Sc. THESIS

**Merve BARDAK
(Y130101020)**

Department of Biomedical Technologies

Thesis Advisor: Prof. Dr. Adnan KAYA

JANUARY 2019

İZMİR KATİP CELEBİ ÜNİVERSİTESİ
FEN BİLİMLERİ ENSTİTÜSÜ

DARBELİ ELEKTROMANYETİK ALANLARIN YÜKSEK
ÇÖZÜNÜRLÜKLÜ KABLOSUZ SENSÖR AĞI İLE
ARAŞTIRILMASI

YÜKSEK LİSANS
Merve BARDAK
(Y130101020)

Biyomedikal Teknolojiler Ana Bilim Dalı

Tez Danışmanı: Prof. Dr. Adnan KAYA

OCAK 2019

Merve BARDAK, a **M.Sc.** student of **IKCU Graduate School Of Natural And Applied Sciences**, successfully defended the thesis entitled “**INVESTIGATION OF PULSED ELECTROMAGNETIC FIELD WITH HIGH RESOLUTION WIRELESS SENSOR NETWORK**”, which she prepared after fulfilling the requirements specified in the associated legislations, before the jury whose signatures are below.

Thesis Advisor :

Prof. Dr. Adnan KAYA
İzmir Katip Çelebi University

.....

Jury Members :

Prof. Dr. Selçuk ÇÖMLEKÇİ
Süleyman Demirel University

.....

Assist. Prof. Dr. Ozan KARAMAN
İzmir Katip Çelebi University

.....

Date of Defense : 31.01.2019



To my family,

FOREWORD

First and foremost, I would like to thank my advisor, Professor Dr. Adnan KAYA, for his encouragement, guidance, support and patience during my M.S. study.

I also would like to thank to Ziyşan Buse YARALI from Biomedical Engineering Department at Izmir Katip Celebi University and Meltem Tezcan for providing and helping in my experiments. At last but not least, I would like to say my grateful thanks to my family for their support and patience during the study.

This thesis was supported by Izmir Katip Celebi University, Coordination Office of Scientific Research Projects.

January 2019

Merve BARDAK

TABLE OF CONTENTS

	<u>Page</u>
FOREWORD	v
TABLE OF CONTENTS	vi
LIST OF TABLES	viii
LIST OF FIGURES	ix
ABBREVIATIONS	xi
ABSTRACT	xii
ÖZET	xiii
ABBREVIATIONS	xi
1. INTRODUCTION	1
1.1 Motivation and Research Objectives.....	1
1.2 Multi-Disciplinary Research	1
2. LITERATURE REVIEW AND BACKGROUND	3
2.1 Theory of Therapeutic Magnetic Field.....	3
2.1.1 Maxwell’s equations for low frequency and high-resolution biomedical problems.....	4
2.2 Electromagnetic Spectrum	5
2.2.1 Biot-savart law	6
2.3 Dielectric Properties of Biological Tissues	7
2.4 Biological Effects of Electromagnetic Fields.....	8
2.4.1 Electric field in multi-layer tissue.....	9
2.5 Literature Review and Historical Background of Wound Healing	11
2.5.1 Wound model and healing mechanism	12
2.5.2 IEEE standard for safety levels with respect to human exposure to electromagnetic field.....	13
2.6 Pulsed Electromagnetic Field and Pulsed Radio Frequency Energy Technologies and Literature Review.....	14
3. PEMF AND PRFE APPLICATOR DESIGN	15
3.1 Material and Methods.....	15
3.2 Coil Model and Geometrical Parameters for PEMF Application	15
3.2.1 Helmholtz Coil Design.....	17
3.3 Antenna Model for PRFE Application.....	19
3.3.1 Flexible Antenna Design Using Kapton Substrate	19
3.3.2 Impedance Matching.....	20
3.4 Results and Discussion.....	21
3.4.1 Simulations and Measurements of Pulsed Electromagnetic Field (PEMF)	21
3.4.2 PRFE Antenna Simulations and Measurement Results	23
4. PEMF AND PRFE EXPOSURE SYSTEM DESIGN, MEASUREMENTS ..	25
4.1 Overview	25
4.2 PEMF Experimental Setup.....	25
4.2.1 PEMF Waveforms.....	28
4.3 Class D Amplifier for PEMF System.....	29
4.4 Active PRFE Experimental Setup	30

4.4.1 Fabrication of Antenna Prototype	31
5. WIRELESS SENSOR NETWORK APPLICAITONS FOR PEMF / PRFE .	34
5.1 Material and Methods.....	34
5.2 Wireless Sensor Network Experimental Setup	34
5.2.1 Wireless Sensor Network Using with Xbee.....	35
5.2.2 Arduino with Pulsed With Modulation.....	38
5.3 Hall Effect Sensor and Measurements	39
5.4 Temperature Sensors and Measurements	40
5.5 E-Health Sensor With in PEMF System	41
5.6 Interface Display with Lattepanda	42
5.6.1 Interface Program for Sensor Applications.....	44
5.7 Comparison of the Sensor Network Measurement and Simulation Result	42
6. PERFORMANCE OF THE PEMF AND PRFE SYSTEMS IN VITRO	
EXPERIMENT.....	46
6.1 Overview	46
6.1.1 Material and Methods	46
6.2 PEMF and PRFE Exposure System	46
6.2.1 Simulations and Biological Results of PEMF and PRFE Exposure to L929 Cells	46
7. CONCLUSION.....	51
REFERENCES.....	53

LIST OF TABLES

	<u>Page</u>
Table 2.1 : Beneficial effects of PEMF therapy in different studies.....	12
Table 2.2 : Basic restrictions applying to various regions of the body [1]	13
Table 2.3 : Electromagnetic field exposure levels in medical applications	14
Table 3.1 : Specifications of designed coil in the PEMF system.....	17
Table 3.2 : Specifications of used antennas in study.....	19
Table 3.3 : Dielectric properties of Kapton.....	20
Table 5.1 : Specifications of sytem equipments.....	35
Table 5.2 : Specifications of DS18B20 Temperature Sensor.....	40



LIST OF FIGURES

	<u>Page</u>
Figure 2.1 : Raditon level of electronic devices.....	5
Figure 2.2 : Straight wire shown to see the magnetic field of a current $d\vec{B}$, at distance r.	6
Figure 2.3 : High water content tissue dielectric properties spectrum.....	7
Figure 2.4 : Action potential of waveform.....	8
Figure 2.5 : Overall PEMF Mechanism	9
Figure 2.6 : The effect of plane wave in fat-muscle model	10
Figure 2.7 : (a) Change of the E-Field (V/m) in the layers of air, muscle and fat (b) Graph of variation of reflection coefficient of air, fat and muscle layers with frequency dispersive material.	11
Figure 3.1 : Magnetic field of coil of wire.....	16
Figure 3.2 : Designed magnetic coils prototypes.....	16
Figure 3.3 : Using the Biot Savart Equations, the flux density B can be found at all points in the coils [29].....	17
Figure 3.4 : The coil design to be used in PEMF systems and the actual PASCO Helmholtz coil views.....	18
Figure 3.5 : Antenna structures at 27.12 MHz.....	19
Figure 3.6 : (a) Flexible Kapton Antenna at 27 MHz (b) Antenna prototype at CST Studio	20
Figure 3.7 : General Matching Condition	21
Figure 3.8 : (a) Antenna matching at CST Studio (b) Antenna of S11 matching and non-matching form.....	21
Figure 3.9 : (a)PEMF system block diagram with petri dish (b) Designed coil with petri dish (c) H- Field on curve along coil to petri dish (d) H field distribution on PEMF system (e) E- Field on curve along coil to petri dish (f) E field distribution on PEMF system.....	22
Figure 3.10 : (a) Helmholtz coil PEMF system block diagram with petri dish (b) Helmholtz coil with petri dish (c) H- Field simulation of the system (d) H field distribution on Helmholtz coil PEMF system (e) E- Field on curve along coil petri dish (f) E field distribution on Helmholtz coil PEMF system	23
Figure 3.11 : Simulation results of the designed antenna at 27.12 MHz (a) Front view of antenna (b) Simulation results of antenna without matching (c) E-field simulation result (d) E-field result through 10 cm line from the antenna (e) H-field simulation result (f) H-field result through 10 cm line from the antenna (g) Simulation result of antenna with matching.	24
Figure 4.1 : Laboratory equipments used in the project	26
Figure 4.2 : PEMF exposure system with designed coil (a) Kikusui Power Generator (b) Exposure of the cell culture to the electromagnetic field (c) FP14000 Class -D Amplifier (d) Arduino sensors (e) Real-time signal display at 75 Hz (f) Measured with Pasco Magnetic Sensor B-Field value at mT.....	27

Figure 4.3 : PEMF exposure System with L929 fibroblast cell line (a) Pasco Helmholtz Coils with sensors (b) Pasco Function Generator (c) LattePanda Display showing sample data received from sensor (d) Arduino system with sensors.....	28
Figure 4.4 : Some of the PEMF / PRFE waveforms in the literature	29
Figure 4.5 : Class D Power Amplifier block diagram	29
Figure 4.6 : FP14000 Class TD Profesional PA Power Amplifier	30
Figure 4.7 : Laboratory equipments used in PRFE exposure system	30
Figure 4.8 : (a) PRFE exposure system (b) Position of the sensors during the experiment	31
Figure 4.9 : (a) FR-4 antenna E-field -18.9 dBm (b) Antenna measurement system with Signal Hound EMC E5 E-Field probe (c) FR-4 matching antenna E-field -15 dBm (d) Antenna measurement system with Signal Hound EMC E5 E-Field probe (e) Kapton matching antenna E-field -14 dBm (f) Antenna measurement system with Signal Hound EMC E5 E-Field	32
Figure 4.10 : (a) FR-4 antenna H-field 15 dBm (b) Antenna measurement system with Signal Hound EMC H20 H-Field probe (c) Kapton antenna H-field 8 dBm (d) Antenna measurement system with Signal Hound EMC H20 H-Field probe	33
Figure 5.1 : (a) System Diagram (b) Arduino – LattePanda connection Arduino – Xbee connection for end device of the wireless network system.....	35
Figure 5.2 : Zigbee system diagram at 2.45 GHz	36
Figure 5.3 : After this simulation we can take the dates graphic about (a) IQ Plot Reference versus Measured (b) Output Spectrum (c) I_Q Half Sine Pulse Shape (d)Data- PRBS- DSSS	37
Figure 5.4 : Pulsed with modulation	39
Figure 5.5 : DRV5053 Analog-Bipolar Hall Effect Sensor	39
Figure 5.6 : (a) (b) DS18B20 Waterproof Temperature Sensor	40
Figure 5.7 : Connection with Arduino in the Sensor Network	41
Figure 5.8 : E-Health Sensor Kit	41
Figure 5.9 : LattePanda with Xbee.....	43
Figure 5.10 : PEMF exposure system with LattePanda	43
Figure 5.11 : Interface program save sensor datas during the experiment	44
Figure 5.12 : (a) Received temperature value is 25.37 °C with DS18B20 sensor (b) and 25.7 °C on petri dish with the infrared sensor.....	45
Figure 6.1 : Wound percent closure area comparison chart.....	48
Figure 6.2 : Microscopic images of PEMF-exposed, PRFE-exposed and control group L929 cell line.....	49

ABBREVIATIONS

AC	: Alternating Current
B	: Magnetic Flux Density
BR	: Basic Restriction
CaM	: Calmodulin
DC	: Direct Current
E	: Electric Field
ELF	: Extremely Low Frequencies
EMF	: Electromagnetic Field
H	: Magnetic Field
ICES	: International Committee on Electromagnetic Safety
iNOS	: Inducible Nitric Oxide Synthase
J	: Induced current Density
nNOS	: Neuronal Nitric Oxide Synthase Isoforms
NO	: Nitric Oxide
NOS	: Nitric Oxide Synthase
PEC	: Perfect Electric Conductor
PEMF	: Pulsed Electromagnetic
PWM	: Pulsed Width Modulation
PRFE	: Pulsed Radio Frequency Energy
RF	: Radio Frequencies
S	: Power Density
SAR	: Specific Absorption Rate
WPAN	: Wireless Personal Area Network
WSN	: Wireless Sensor Network

INVESTIGATION OF PULSED ELECTROMAGNETIC FIELD WITH HIGH RESOLUTION WIRELESS SENSOR NETWORK

ABSTRACT

Several studies demonstrate the healing properties of pulsed electromagnetic fields. The healing properties of electromagnetic field treatments have been observed in various tissues such as bone, soft and cancer tissue. Pulsed electromagnetic fields, considering as electromagnetic excitation without side effects because of their low energy level, affect body tissues and increase the permeability of cell membranes. It is accepted that the ionic activities of the tissues help the treatment by accelerating the blood circulation. The pulsed electromagnetic fields have variant effects on biological tissues of various waveforms, amplitude and duration of exposure time at different frequencies.

Although Wireless Sensor Network (WSN) technology, using numerous innovative applications, it is still not widely used in electromagnetic field experiments. In this study, magnetic field and temperature measurements were made by WSN technology. In addition, cell culture temperature and magnetic field changes of Pulsed Electromagnetic Field and Pulsed Radio Frequency exposure system were observed. The main purpose of this research is to innovate the usual PEMF and PRFE studies using WSN technology and to continue wound healing studies more effectively. During PEMF and PRFE applications, magnetic field and temperature gradients with sensors are observed. Different types of antennas and coils are designed and analyzed for pulsed electromagnetic field processing systems. Antennas and test devices designed for PRFE system were modelled and simulated with biological tissues using CST Microwave Studio. Similarly, system simulations were performed with biological tissues in coils designed for PEMF system. To prevent sensor data loss, interface program and implement real-time environmental data collection platform was designed.

To summarize, three different mechanisms were compared with the wound healing effects of PEMF, PRFE and control group on L929 fibroblast cell culture. As a result, it is determined that depending on the frequency and magnetic flux density parameters of PEMF and PRFE applications can increase and accelerate cell proliferation.

DARBELİ ELEKTROMANYETİK ALANLARIN YÜKSEK ÇÖZÜNÜRLÜKLÜ KABLOSUZ SENSÖR AĞI İLE ARAŞTIRILMASI

ÖZET

Darbeli elektromanyetik alanların iyileştirici özelliklerini gösteren birçok çalışma vardır. Elektromanyetik alan tedavilerinin iyileştirici özellikleri kemik, yumuşak ve kanser dokusu gibi çeşitli dokularda gözlenmiştir. Darbeli elektromanyetik alanlar, yan etkileri olmayan ve düşük enerji seviyelerinden dolayı zarar vermeyen elektromanyetik uyarma olarak kabul edilir. Dokuların iyon aktivitelerini, kan dolaşımını hızlandırarak tedaviye yardımcı olduğu kabul edilir. Darbeli elektromanyetik alan tedavisi farklı frekanslarda, dalga formlarında, genlikte ve maruz kalma süresinde biyolojik dokular üzerinde değişken etkilere sahiptir. Hızla birçok alanda kullanımı yaygınlaşan Kablosuz Sensör Ağı teknolojisi sayısız yenilikçi uygulamaya sahip olmasına rağmen hala elektromanyetik alan deneylerinde kullanımı yaygın değildir.

Bu çalışmada, Kablosuz Sensör Ağı teknolojisi ile manyetik alan ve sıcaklık ölçümleri yapılarak, hücre kültürünün sıcaklık değişimleri ve Darbeli Elektromanyetik Alan uygulamasının manyetik alan değişimleri gözlemlenmiştir. Bununla birlikte, Darbeli Elektromanyetik Alan/Darbeli Radyo Frekans uygulamaları boyunca hücre kültüründe sıcaklık ve uygulanan manyetik alanda değişimler gözlemlenmiştir.

Bu çalışmanın temel amacı, Kablosuz Sensör Ağı teknolojisi ile 27.12 MHz taşıyıcı frekansında ve Darbeli Elektromanyetik Alan uygulamalarında 75 Hz'de biyolojik dokular üzerinde in-vitro deneylerle yara iyileşmesini araştırmaktır. Darbeli Elektromanyetik Alan ve Darbeli Radyo Frekans uygulamaları sırasında manyetik alan ve sıcaklık değişimleri sensörler ile gözlemlenmiştir. Darbeli elektromanyetik alan uygulamaları için farklı tip antenler ve bobinler tasarlanmış ve analiz edilmiştir.

Tez çalışmam süresince, CST Microwave Studio kullanılarak biyolojik dokular üzerinde sistem analiz edilmiştir. Ayrıca, Darbeli Radyo Frekans Uygulaması için tasarlanan antenler ve test cihazları CST Microwave Studio kullanılarak biyolojik dokularla modellenip simülasyonları yapılmıştır. Benzer şekilde, Darbeli Elektromanyetik Alan sistemi için tasarlanan bobinlerde biyolojik dokularla sistem simüle edilmiştir. Sensörlerden toplanan veri kaybını önlemek amacıyla, arayüz programı ve gerçek zamanlı çevresel veri toplama platformu tasarlanmıştır.

Bu çalışmalar sonucunda elde edilen bulgularda, kontrol grubunun yara iyileşme etkileriyle L929 fibroblast hücre kültürü üzerindeki üç farklı sistem ile karşılaştırılmıştır. Sonuç olarak, darbeli elektromanyetik alan uygulamalarının, frekans ve manyetik akı yoğunluğu parametrelerine bağlı olarak hücre çoğalmasımı arttırdığı ve hızlandırdığı tespit edilmiştir.

1. INTRODUCTION

1.1 Motivation and Research Objectives

Pulsed magnetic field treatments are applied as an adjunctive treatment [1]. The ions in each tissue in the body are affected by the change of electromagnetic fields around them during their biochemical activities. Non-thermal low electromagnetic fields can be transferred to the tissues by electromagnetic field application. It has been reported in many studies that this has a therapeutic, healing-accelerating effect. The main topic of this study is to investigate the role of pulsed electromagnetic field (PEMF) and pulsed radiofrequency (PRFE) applications in wound healing by using high resolution wireless sensor network network (WSN). In addition, it is to develop a study that operates on the 27.12 MHz band, which produces low level electromagnetic energy, and particularly increases wound healing and to find the most efficient system with simulations make design the experimental setup according to these data and investigate the effects on wound healing. In order to be used in PRFE applications, it is aimed to simulate a flexible antenna which is compatible with biomedical studies and then to produce the antenna. For the purpose of bringing a difference and innovation to the study, the experimental setup with WSN technology was combined. The magnetic field and temperature sensors placed near the cell line during the experiment showed the effects of the applied electromagnetic field on the cell line. The temperature of the cell line in the cell culture dishes was also measured by the infrared temperature sensor. The sensor contents collected during the 4-hour test were recorded in the interface program.

1.2 Multi-Disciplinary Research

In this thesis, the methods we have applied and the details of the departments:

Chapter 1 presents the purpose and method of the research are explained. The details of the works carried out in each section are summarized.

Chapter 2 is based on the basic principles of electromagnetic applications, the principles of interaction of biological tissues from the electromagnetic field is the main subject of this chapter. In addition, examples of various PEMF and PRFE applications and exposure limits in these applications are given in the literature.

Chapter 3 simulates the Helmholtz coil system and the designed coil system, which can produce uniform magnetic flux at 75 Hz in the PEMF system, for in vitro experiments before designing experimental setup system prototypes. Likewise, the antenna design of the PRFE system, designed for the same purpose, was simulated for in vitro experiments at 27 MHz. The uniformity region was determined by these experiments.

Chapter 4, in order to observe wound healing in tissues, three system assemblies have been established. In the first, the PEMF system is designed to form a homogeneous time-varying 4 mT electromagnetic field. The second PEMF system is designed with Helmholtz coil and 1 mT electromagnetic field is created. In the PRFE system, a 7 mT electromagnetic field was created with a matching antenna. Wound healing performance in L929 fibroblast cells was also investigated in amplified systems.

Chapter 5 presents wireless sensor network. The sensors we use are described in this section of arduino systems, the receiver circuit and the designed interface program.

Chapter 6 presents in vitro studies with PEMF/ PRFE exposure system. L929 cell line wound healing rates, the results of the experiment and the interpretation was made.

Chapter 7 evaluation, contributions and summary of the results of the research are presented. With this study, the PEMF system designed with 1 mT Helmholtz Coil proved the most effective wound healing on the cell line.

2. LITERATURE REVIEW AND BACKGROUND

2.1 Theory of Therapeutic Magnetic Field

Studies of the magnetic field with biological system has a long history. The oldest document in this field is the bioelectric events that describe the electric sheatfish in the Egyptian hieroglyph of 4000 B.C. The first written document on the electrotherapeutic is recommended the use of torpedo fish for headaches and gouty the year A.D. 46 when Scribonius Largus [2]. But the first known techniques today electromagnetic field application with equipments started in the 1700s. Galvani and Volta (1700s) experimented with electrical effects in frog's legs [kitab]. In the 1800s, scientists such as Gauss, Weber, Faraday and Maxwell had made the basis of modern electricity and magnetism. Using electric field heating for control of cancer by Recamier and Pravaz in the destruction of uterine cancer in the 1800s [3]. D'Arsonval research the effect of low-frequency currents on electrophysiological activity in muscles and nerves (1896) [2]. In 1898 Nicola Tesla first introduced the principle of Pulsed Electromagnetic Field therapy. Additionally, magnetotherapy has a long history in Europe. When 1864, the electromagnetic connection was theoretically formulated and developed equations that time-varying electricity and magnetism [4]. The first clinical application of electromagnetic stimulation in the USA by Basset in 1977. After that, the first magnetotherapy book was written by Todorov in 1982. There have been many clinical applications in this area, especially in Asia and Europe. In the last three decades, a large number of studies have proved that EMFs have multiple effects to living organisms[5-8].

2.1.1 Maxwell's equations for low frequency and high-resolution biomedical problems

The behavior of time-varying, static electric and magnetic fields are formulated by James Clerk Maxwell [4]. These equations simply summarize the mathematical consequences of the classical experiments of Faraday, Ampere, Coulomb, Maxwell, and others.

$$\vec{\nabla}_x \vec{E} = -\vec{M}_i - \frac{\partial \vec{B}}{\partial t} \quad (2.1)$$

$$\vec{\nabla}_x \vec{H} = \vec{J}_i + \vec{J}_c + \frac{\partial \vec{D}}{\partial t} \quad (2.2)$$

$$\vec{\nabla} \cdot \vec{D} = q_{ev} \quad (2.3)$$

$$\vec{\nabla} \cdot \vec{B} = 0 \quad (2.4)$$

$$\vec{\nabla} \cdot \vec{B} = 0 \quad (2.5)$$

Equation (2.1) is a statement of Faraday's law; time-varying magnetic field induces an electric field. Equation (2.2) is a statement of Ampere's law that the line integral of magnetic field around a closed loop equals the total current through the loop. Equation (2.3) arises from Coulomb's law and relates the electric displacement to the sources that generate it, namely the charge density. Equation (2.4) recognizes that no magnetic charges exist, and hence the magnetic induction, must be solenoidal. Equation (2.5) is a statement of the conservation of charge, namely that its outflow from any closed region can arise only if the charge contained is depleted.

$$\oint_c \vec{E} \cdot \vec{dl} = - \iint \vec{M}_i \cdot \vec{ds} - \frac{\partial}{\partial t} \iint \vec{B} \cdot \vec{ds} \quad (2.6)$$

$$\oint_c \vec{H} \cdot \vec{dl} = \iint_s \vec{J}_i \cdot \vec{ds} + \iint_s \vec{J}_c \cdot \vec{ds} + \frac{\partial}{\partial t} \iint_s \vec{D} \cdot \vec{ds} \quad (2.7)$$

$$\oiint_s \vec{D} \cdot \vec{ds} = Q_e \quad (2.8)$$

$$\oiint_s \vec{B} \cdot \vec{ds} = 0 \quad (2.9)$$

$$\oiint_S \vec{J}_{ic} \cdot d\vec{s} = -\frac{\partial}{\partial t} \iiint_V q_{ev} \cdot d_v = \frac{\partial Q_E}{\partial t} \quad (2.10)$$

2.2 Electromagnetic Spectrum

The electromagnetic spectrum is a measure of the range of all types of EM radiation. The other types of EM radiation that make up the electromagnetic spectrum are microwaves, infrared light, ultraviolet light, X-rays and gamma-rays. Wave has a few fundamental properties that describe it. Frequency; measured in Hertz, which counts the number of waves that pass by a point in one second and wavelength; the distance from the peak of one wave to the peak of the next. These two attributes are inversely related. Waves with longer wavelengths have lower frequencies because of fewer wave peaks cycle per second.

The biological effects of electromagnetic waves exposure to excessive levels of electromagnetic power over prolonged periods can cause adverse health effects. General exposure limits are set by the World Health Organisation (WHO). Biological effect of exposure to electromagnetic power is critical for therapeutic application.

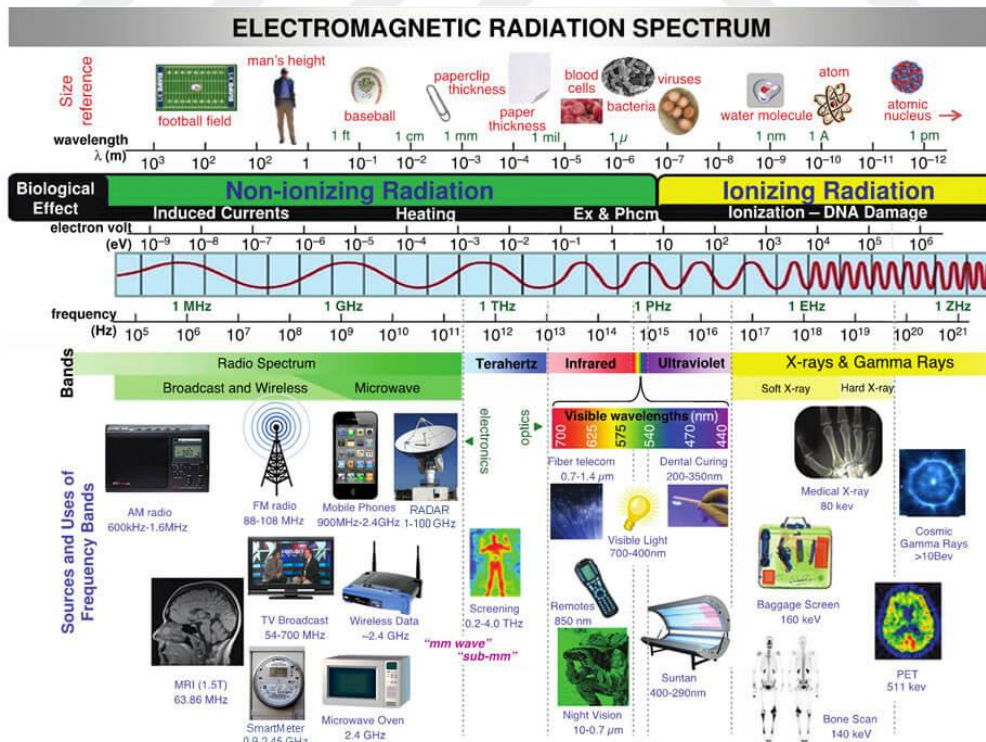


Figure 2.1 : Raditon level of electronic devices.

As graphic shows, EMR comes in two types: ionizing and non-ionizing. Ionizing radiation is carrying enough energy to break chemical bonds into ions and therefore potentially damage DNA (Figure 2.1). Non-ionizing radiation does not carry enough energy to ionize molecules.

2.2.1 Biot-savart law

Biot- Savart Law equations are describing the magnetic field generated by a constant electric current. It relates the magnetic field to the magnitude, direction, length of wire, and proximity of the electric current. The equation used to calculate the magnetic field generated at some arbitrary point P by a steady current. The law is named for Jean-Baptiste Biot and Felix Savart, who first formulated this relationship in 1820.

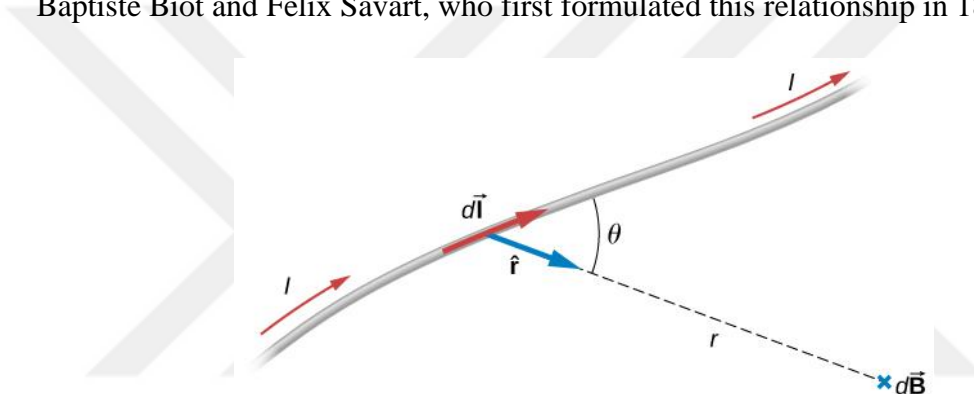


Figure 2.2 : Straight wire shown to see the magnetic field of a current $d\vec{B}$, at distance r .

That at any point P, the magnetic field $d\vec{B}$ due to an element $d\vec{l}$ of a current-carrying wire is given by (Figure 2.2)

$$d\vec{B} = \frac{\mu_0 I d\vec{l} \times \hat{r}}{4\pi r^2} \quad (2.11)$$

The constant μ_0 is known as the permeability of free space and is exactly

$$\mu_0 = 4\pi \times 10^{-7} T \cdot m/A \quad (2.12)$$

The infinitesimal wire segment $d\vec{l}$ is in the same direction as the current I (assumed positive), r is the distance from $d\vec{l}$ to P and \hat{r} is a unit vector that points from $d\vec{l}$ to P , as shown in the figure. The direction of $d\vec{B}$ is determined by applying the right-hand rule to the vector product $d\vec{l} \times \hat{r}$. The magnitude of $d\vec{B}$

$$dB = \frac{\mu_0 I dl \sin \theta}{4\pi r^2} \quad (2.13)$$

$$B = \nabla \times A = \nabla \times \frac{\mu_0 I}{4\pi} \int \frac{ds}{R} \quad (2.14)$$

2.3 Dielectric Properties of Biological Tissues

Electromagnetic field with biological tissue, it is important to know its complex permittivity to understand the interaction of the (Staebell, et.al., 1990). Researches shows about the dielectric properties of biological tissue the dielectric properties and penetration depth in the tissue are strongly correlated with its water content (Figure 2.3) [11]. Hence, depending on the type of tissue, if it is mainly composed of water, such as brain, muscle and skin, the EM-waves are attenuated considerably before they reach the receiver due to their high permittivity and loss [12-13].

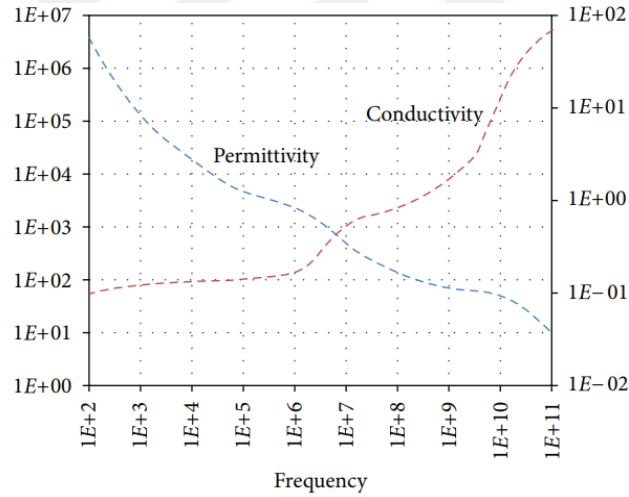


Figure 2.3: High water content tissue dielectric properties spectrum.

The fundamental electrical property through which the interactions are described is the complex relative permittivity of the material ϵ^* . Mathematically expressed as [14]

$$\epsilon^* = \epsilon' - j\epsilon'' \quad (2.15)$$

where ϵ' = dielectric constant and ϵ'' = dielectric loss factor. The absolute permittivity of a vacuum, ϵ^0 is determined by using the relation [14]

$$C_0\mu_0\epsilon^0 = 1 \quad (2.16)$$

C_0 = speed of light (3×10^8 m/ s.), μ_0 = magnetic permeability (1.26×10^{-6} H/m.) and ϵ^0 = absolute permittivity of a vacuum (8.854×10^{-12} F/m) [14]

Sanjeev Kumar et. al, (2010) have developed a MATLAB program which computes the dielectric parameters such as dielectric constant, loss, loss tangent, conductivity, penetration depth and attenuation factor is with Microsoft Excel to develop a combined program in MATLAB that makes a determination of T and τ [15].

2.4 Biological Effects of Electromagnetic Fields

The influence of electromagnetic fields on tissues is a well-known subject for many years. The main subject of the research is how it affects tissues and how these effects change in every changing parameter. Although it is not completely known how the electromagnetic fields affect the tissues, there are studies about intracellular effects. In this direction, researches show when a cell is excited and ionic currents begin to flow results consecutive depolarization and repolarization (Figure 2.4). When a cell is stimulated flow results depolarization and repolarization. In the meantime cause changes in the levels of mRNA and protein synthesis, alteration of cellular membrane's permeability, and Ca^{2+} , Na^+ , K^+ ion transfer. Therefore influence the differentiation of primitive stem cells, and alter the rates of apoptosis in both normal and neoplastic cells [8, 16-18]. Looking at their effects at the molecular level influence the expression of early-induced genes such as c-myc, c-fos, c-jun, and they affect synthesis of various proteins, among them, the tumour suppressor protein P53 [8].

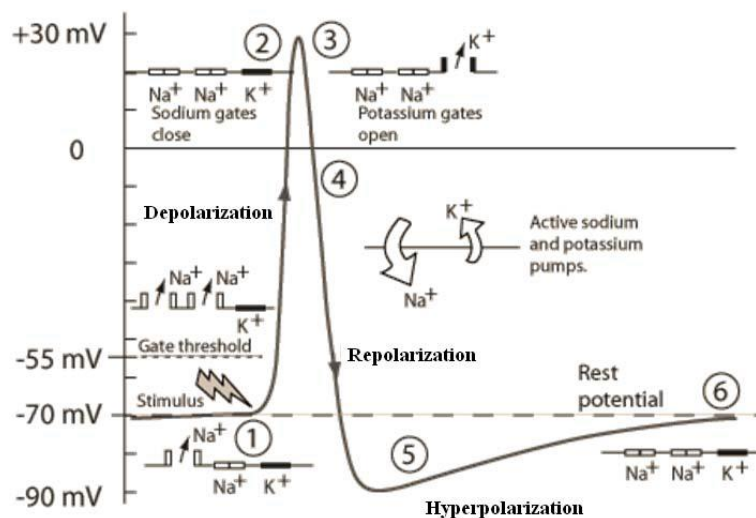


Figure 2.4 : Action potential of waveform.

To summarize the work done about effects PEMF on cell: increases oxygen level, promotes blood circulation, triggers the production of adenosine triphosphate, enhances membrane permeability, ion transfer and cell metabolism, promotes cellular curing, improves communication between cells, promotes the transfer of ions in cells.

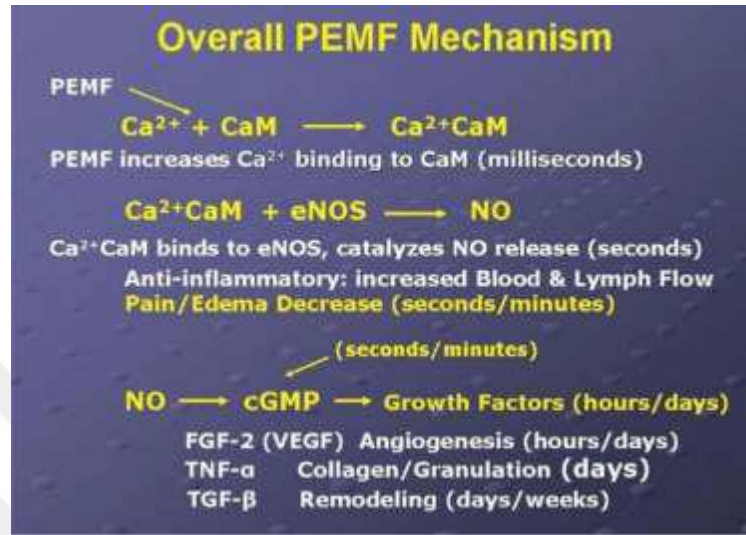


Figure 2.5: Overall PEMF mechanism.

According to this proposed mechanism CaM, NOS, and cGMP inhibitors that individually eliminated the PEMF effect on DNA synthesis [19]. At the cellular level interaction EMF signal transduction pathway relevant to tissue maintenance, repair and regeneration begin with Ca^{+2} binding to CaM (Figure 2.5). Direct effect of a PEMF signal configured for the Ca and CaM pathway on real-time NO production in a neuronal cell line, which could be eliminated by CaM and NOS inhibitors, has also shown.

2.4.1 Electric field in multi-layer tissue

Biological tissues are lossy materials so this loss changes the way the wave interacts with the material and its propagation behavior. Therefore, the reflection and transmission properties vary in different multi-layered tissue. As shown in Fig.2.6 the transmitted wave perpendicular to the boundary interacts with the reflected wave. The result of the modification of the reflection and transmission coefficients, many

reflections occur between tissue boundaries. During the EM power passes through lossy material, thus causing loss to the propagating wave.

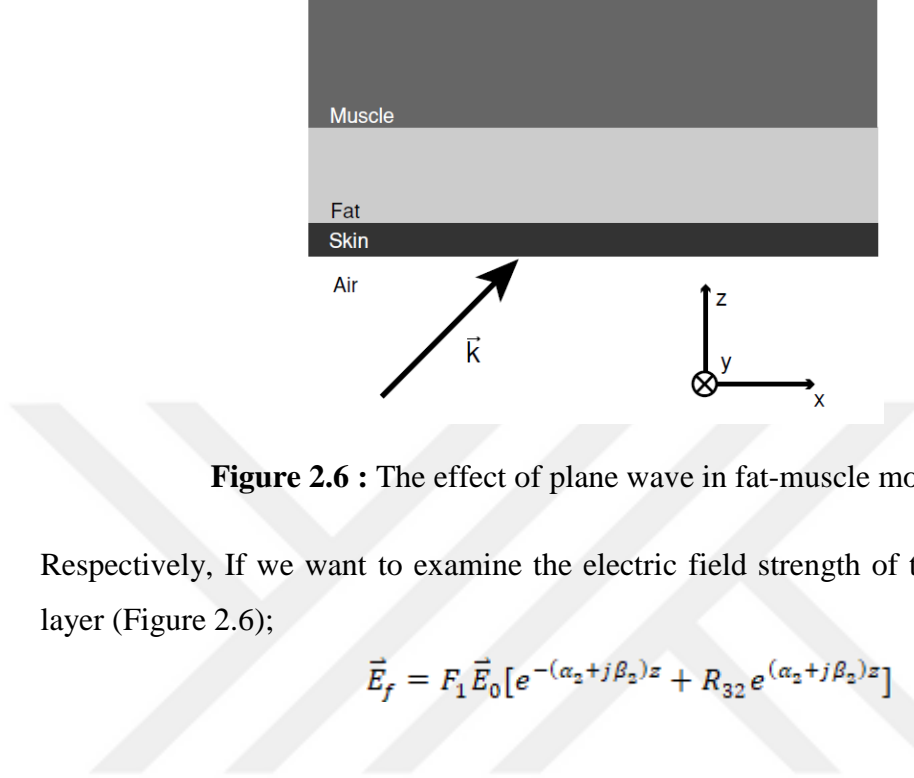


Figure 2.6 : The effect of plane wave in fat-muscle model.

Respectively, If we want to examine the electric field strength of the layers, for fat layer (Figure 2.6);

$$\vec{E}_f = F_1 \vec{E}_0 [e^{-(\alpha_2 + j\beta_2)z} + R_{32} e^{(\alpha_2 + j\beta_2)z}] \quad (2.17)$$

In addition, the second layer of electric field in the underlying muscle tissue is given by

$$\vec{E}_m = F_t \vec{E}_0 e^{-(\alpha_3 + j\beta_3)z} \quad (2.18)$$

Here α_2, β_2 are the attenuation and propagation coefficients in fat layer and α_3, β_3 are also in muscle layer. The layer function F and the transmission function T are given by

$$F_1 = F_{12} / [e^{-(\alpha_2 + j\beta_2)l} + R_{12} R_{32} e^{-(\alpha_2 + j\beta_2)l}] \quad (2.19)$$

$$F_t = T_{12} T_{23} / [e^{(\alpha_2 + j\beta_2)l} + R_{21} R_{32} e^{-(\alpha_2 + j\beta_2)l}] \quad (2.20)$$

Where l is the thickness of adipose tissue and T_{12} is transmission coefficients at the air-fat boundaries. T_{23} is referred to transmission coefficients fat-muscle boundaries. R_{12} and R_{32} is the reflection coefficient for these boundaries. The reflection

coefficient and magnitude of the electric field in different layers of different thicknesses at these limits were calculated. In these calculations, the thickness of the fat tissue was taken as 10 mm and the thickness of the muscle tissue was taken as 28 mm (Figure 2.7).

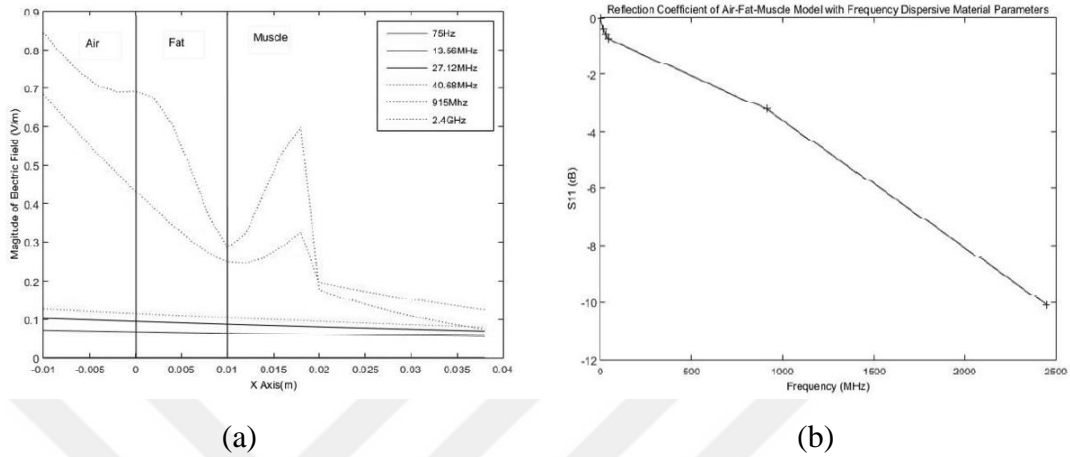


Figure 2.7: (a) Change of the E-Field (V/m) in the layers of air, muscle and fat (b) Graph of variation of reflection coefficient of air, fat and muscle layers with frequency dispersive material.

2.5 Literature Review and Historical Background of Wound Healing

Therapy with EMF has been used for quite a long time in several therapeutic aims, and the efficacy of low-intensity EMFs has been demonstrated in several clinical applications literature. A large number of studies show that EMFs have multiple effects to living organisms [5-8]. Clinical applications include various treatment such as fractures, wounds healing, heart disease and headache disorders. In this study, we focused on non-ionizing low frequency pulsed electromagnetic fields the therapeutic effects on wound healing. The waveform of PEMF can be rectangular, sinusoidal, biphasic and quasitriangular in shape [20]. Specific types of low-level EMFs have the ability to produce specific responses, depending on the parameters such as magnitude, frequency, the waveform of the field [21]. Some of the studies with the application of PEMF radiation to damaged skin have shown that can accelerate re-establishment of normal potentials and thereby facilitate the process of wound.

Table 2.1: Beneficial effects of PEMF therapy in different studies.

Study	Parameters	Effect of MF
Stiller et al. [22]	PELUT; $\Delta B = 2.2$ mT; 3 part pulse (+, -, +) of 3.5 msec total width 3 hrs daily; 8 weeks (or earlier is healed); 12 wks total if improvement present at 8 wks	Decreased wound depth and pain intensity
Omote et al. [23](Rats) (Cell culture)	4 mT, 200 Hz, pulse width 2.0 msec 1 hr (once) 4 mT, 250 Hz, pulse width 1.5 msec 2 hrs (once)	Increased survival of rats; survival greatest when PEMF and drug given in combination Colony formation suppressed; greater suppression with Combination PEMF & drug
Ieran et al. [24]	2.8 mT, 75 Hz, 1.3 msec 3-4 hrs daily; 90 days	Increased success rate of treating venous skin ulcers; reduced recurrence rate

2.5.1 Wound model and healing mechanism

There are different theories that may explain the effects of EMFs procedure of tissue regeneration and cell proliferation. Studies show that there is a cellular dimensional interaction. As detailed in the previous section at the cellular level interaction EMF signal transduction pathway relevant to tissue maintenance, repair and regeneration begin with Ca^{+2} binding to CaM. Also ROS (free radical) is an important mechanism involved in the wound healing process, and free radicals play a role in the elimination of damaged cells. In this case, free radical atoms (superoxide anion $[O-2]$ and hydroxyl anion $[OH-]$) which are exemplary molecules for ROS they will be affected by a magnetic field. It is envisaged that the EMFs mechanism can regulate the balance of ROS and antioxidants. Examples of this effect include Na^+ , Cl^- , Ca^{+2} and K^+ ions. It supports these predictions in the studies in the literature. Theories suggest that the primary actions of EMFs are correlated with the production of small quantities of free radicals within cells [25,26].

2.5.2 IEEE standard for safety levels with respect to human exposure to electromagnetic field

The electromagnetic field might cause harmful effects to the human health. National and international committees have studied some methods to evaluate the potential damage of the electromagnetic fields. Various organizations have prepared a maximum permissible exposure level of humans exposed to RF electromagnetic radiation guidelines to prevent damage from these exposures. ICES (International Committee on Electromagnetic Safety) Technical Committee 95 (TC95) is responsible for these standards [27]. There are five TC95 subcommittees in a range of 0 Hz to 300 GHz.

The basic restrictions of the electric field applied on a 5 mm long straight line directed in any direction within the tissue described in the frequencies in the range 0 to 5 MHz (Table 2.2). The average time for rms measurement was taken as 0.2 s.

Table 2.2: Basic restrictions applying to various regions of the body [36].

Exposed tissue	f_e (Hz)	General public	Controlled environment
		E_0 . rms (V/m)	E_0 . rms (V/m)
Brain	20	5.89×10^{-3}	1.77×10^{-2}
Heart	167	0.943	0.943
Hands, wrist, feet and ankles	3350	2.10	2.10
Other tissue	3350	0.701	2.10

To summarize the exposure levels of electromagnetic field applications for medical applications are shown in this Table. The purpose of this standard is to provide protection against the adverse effects of high electromagnetic fields and radio frequencies.

In addition, animal studies show that does not cause a temperature increase unless RF exposure $> 4 \text{ W / kg}$ and does not adversely affect the reproductive and developmental effects of the subjects.

Table 2.3: Electromagnetic field exposure levels in medical applications.

Source	Frequency	Distance	Exposure	Remarks
Shortwave diathermy	27.12 MHz	0.2m	$<1000 \text{ V}\cdot\text{m}^{-1}$	Staff exposed
		0.5 m	$<500 \text{ W}\cdot\text{m}^{-2}$	Patient, untreated body parts
		1 m	$<140 \text{ V}\cdot\text{m}^{-1}$ $100\text{-}1000 \text{ V}\cdot\text{m}^{-1}$	Staff
Microwave treatment	433 MHz	0.5 m	$25 \text{ W}\cdot\text{m}^{-2}$	Patient, untreated body parts
		1 m	$10 \text{ W}\cdot\text{m}^{-2}$	
		0.3-3 m	$50\text{-}200 \text{ W}\cdot\text{m}^{-2}$	Whole body average
Magnetic Resonance Imaging (MRI)	433 MHz	Within system	$20\text{-}140 \text{ W}\cdot\text{m}^{-2}$	Frequency depending on the static field
	2450MHz			SAR refers to normal operational mode
	42-300 MHz		up to $2 \text{ W}\cdot\text{kg}^{-2}$	

2.6 Pulsed Electromagnetic Field and Pulsed Radio Frequency Energy Technologies and Literature Review

Pulsed electromagnetic fields, which have a wide usage area in medicine, have a positive effect on the healing process when used as adjunctive therapy. Another application of electromagnetic field, which can be used in wound healing, is PRFE application at 27.12 MHz carrier frequency. Pulsed RF energy has a wide range of therapeutic uses and it is verified by performing a Specific Absorption Rate (SAR) evaluation have no negative effects on human health. For this reason, there are different application examples of PRFE treatment in different waveforms.

3. PEMF AND PRFE APPLICATOR DESIGN

3.1 Material and Methods

The use of antennas and coils for therapeutic purposes in medical applications has been one of the popular research topics of recent times. In the light of the researches in the literature, the mechanisms designed with new methods are presented in this section. The most efficient wound healing method was investigated with three different systems designed and the findings were presented. 2-axis uniform magnetic field with time varying Helmholtz coil designed with high magnetic field producing coil systems are compared. The system simulations of the antenna which is designed and produced in accordance with medical experiments made of flexible kapton material were made. In this section, the simulations of these three main systems are examined for the most efficient results.

3.2 Coil Model and Geometrical Parameters for PEMF Application

It is particularly interesting to compare the field from Helmholtz coils at the proper separation of the coil radius to the field from coils separated at less than or more than the coil radius. The magnetic field inside a single coil can be examined in both the radial and axial directions [28]. The magnetic field intensity is directly proportional to the number of turns and the current through the coil. Based on the right-hand rule, fields perpendicular to the common axis cancel each other and parallel fields in the same direction are mutually intensifying. This results in uniform magnetic field in the area between the bobbins.

For a coil of wire having radius R and N turns of wire, the magnetic field along the perpendicular axis through the center of the coil is given by Formula 3.1.

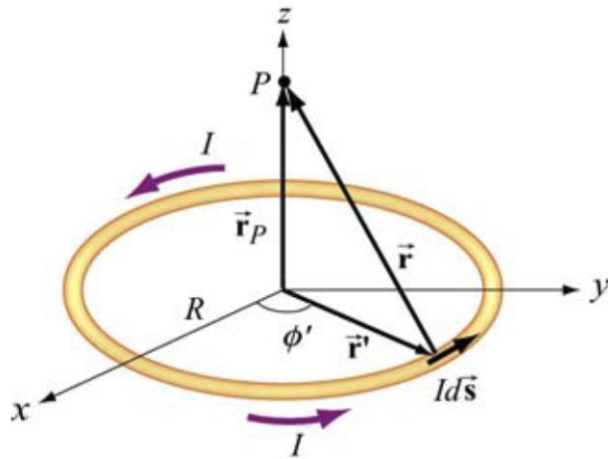


Figure 3.1: Magnetic field of coil of wire.

$$B = \frac{\mu_0 N I R^2}{2(p^2 + R^2)^{3/2}} \quad (3.1)$$

I : coil current (A)

B : magnetic field (Gauss)

N : number of turns of wires on each coil

μ_0 : Permeability of free space $4\pi \times 10^{-7} \text{ H/m}$

R : radius of coils (cm)

x : distance from a point of observation

Different types of coils with different shapes create different electric fields (Figure 3.2). For this reason, it has been recognized that coil size, number of turn and shape. The results show that these parameters play an important role in the efficiency of the simulations and therefore in the subsequent experiments.



Figure 3.2: Designed magnetic coils prototypes.

In these cases, a coil provides a uniform magnetic field intended. We chose the coil which one would be the most efficient in this project. The specifications of the coil are shown in detail in the (Table 3.1).

Table 3.1: Specifications of designed coil in the PEMF system.

DC	AC	D. Cyle	V _{OUT}	I _{OUT}	Volt-Amper	Simulation (mT)	Measurement (mT)
3	3	10	29	0,77	22,44	1,51	1,5
3	3	25	60,44	1,61	97,45	3,16	3,4
3	3	50	80	2,13	170,74	4,18	4,8
3	4	10	36	0,96	34,57	1,88	1,8
3	4	25	73	1,95	142,17	3,76	4,1
3	4	50	98	2,61	256,21	5,12	5,5
2	4	10	46	1,23	56,45	2,41	2,25
2	4	25	103	2,75	283,03	5,4	5,65
2	4	50	136	3,63	493,43	7,12	7,55

3.2.1 Helmholtz Coil Design

The main purpose of Helmholtz coils systems used in medical applications is to produce an almost homogeneous magnetic field. For this purpose, the coils consist of identical coils. The magnetic field strength depends on two main parameters, the number of coils and the current. For this reason, the coils positioned symmetrically on the same axis carry an equal amount of current in the same direction. This positioning ensures a uniform magnetic field at the very center [29]. The formation of a uniform magnetic field between the coils is dependent on the areas perpendicular to the common axis and the parallel fields in the same direction, canceling each other. It is based on the right hand rule.

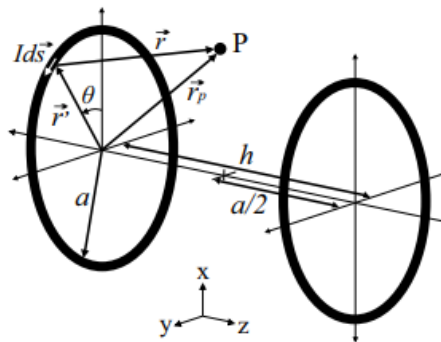


Figure 3.3 : Using the Biot Savart Equations, the flux density B can be found at all points in the coils [29].

$$B = \nabla \times A = \nabla \times \frac{\mu_0 I}{4\pi} \int \frac{ds}{R} \quad (3.2)$$

μ_0 : permeability of free space $4\pi \times 10^{-7} \text{ H/m}$

I : coil current (A)

∇ : gradient

ds : infinitesimal segment of the current loop

R : distance from a point of observation

For the coil having N number turns, the expression for magnetic field along the axis due to both the coils is

$$B(z) = \frac{1}{2} \mu_0 N I R^2 \left\{ \left[R^2 + \left(z + \frac{R}{2} \right)^2 \right]^{-3/2} + \left[R^2 + \left(z - \frac{R}{2} \right)^2 \right]^{-3/2} \right\} \quad (3.3)$$

At the center of Helmholtz coil ($z = 0$), the magnetic field intensity is

$$B(0) = \frac{16}{5\sqrt{5}} \frac{1}{2} \frac{\mu_0 N I}{R} = 1.43 * \frac{\mu_0 N I}{D} \quad (3.4)$$

B : magnetic field (*Gauss*)

R : radius of coils (*cm*)

N : number of turns of wires on each coil

I : current through each turn of wire (A)

In view of these situations there is a need for a coil system that provides an almost homogeneous magnetic field targeted and is easy to use in experiments. The Helmholtz coils selected and used for this study is shown in Fig 3.4.



Figure 3.4: The coil design to be used in PEMF systems and the actual PASCO Helmholtz coil views.

3.3 Antenna Model for PRFE Application

In this study, rectangular and octagonal spiral antennas were designed to transmit the PRFE signal at 27.12 MHz. After the antenna has been designed in free space conditions, it is redesigned by optimizing the dimensions, supply lines and other parameters in the antenna by finding the best base with biological materials. The antennas are designed on FR4 material with a resonance frequency of 27.12 MHz. Figure shows the geometry of antennas at CST Studio. In addition to these, an antenna of flexible Kapton material is designed and manufactured.

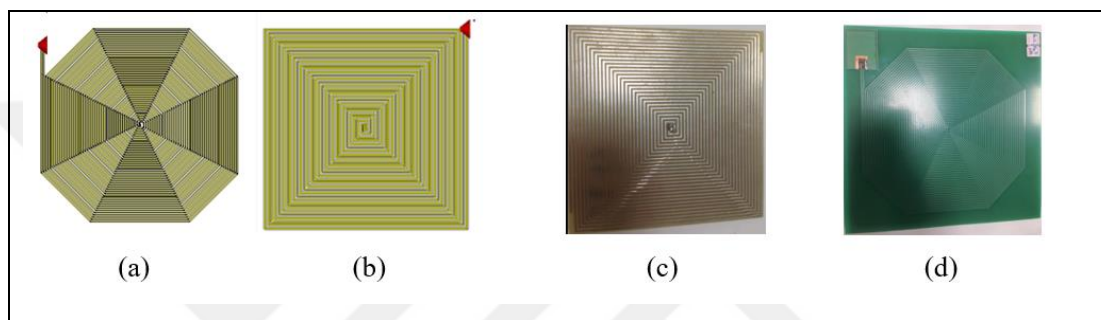


Figure 3.5: Antenna structures at 27.12 MHz.

Design and construction of the antennas used for this study (Figure 3.5). CST Studio simulations are based on the properties of the materials used in the antennas (Table 3.2).

Table 3.2: Specifications of used antennas in study.

Substrate of Antenna	FR4	Kapton
Dielectric Constant	4,3	4
Tangential Loss	0,001	0,005
Dielectric Thickness	1,6 mm	0,15 mm
Dielectric Thickness	0,6 mm	0,35 mm

3.3.1 Flexible Antenna Design Using Kapton Substrate

To make the designed antenna suitable for implantation, it is embedded in biocompatible Kapton. Kapton is a polyimide film, which possesses excellent physical, electrical, and mechanical properties over a wide temperature range. Typical applications for Kapton polyimide film include wire and cable tapes, formed coil and magnet wire insulation, and transformer and capacitor insulation.

Table 3.3: Dielectric properties of Kapton.

Parameter	Specification
Grade	H
Thickness (mil)	1
Dielectric Constant	3,4
Dissipation Factor (x104)	18
Dielectric Strength (kV/mil)	7,7
Long Term Temp. (°C)	-269 to 400
Shrinkage (%)	0,17-1,25
Density (g/cc)	1,42

The prototype of the Kapton antenna with the features given (Table 3.3).

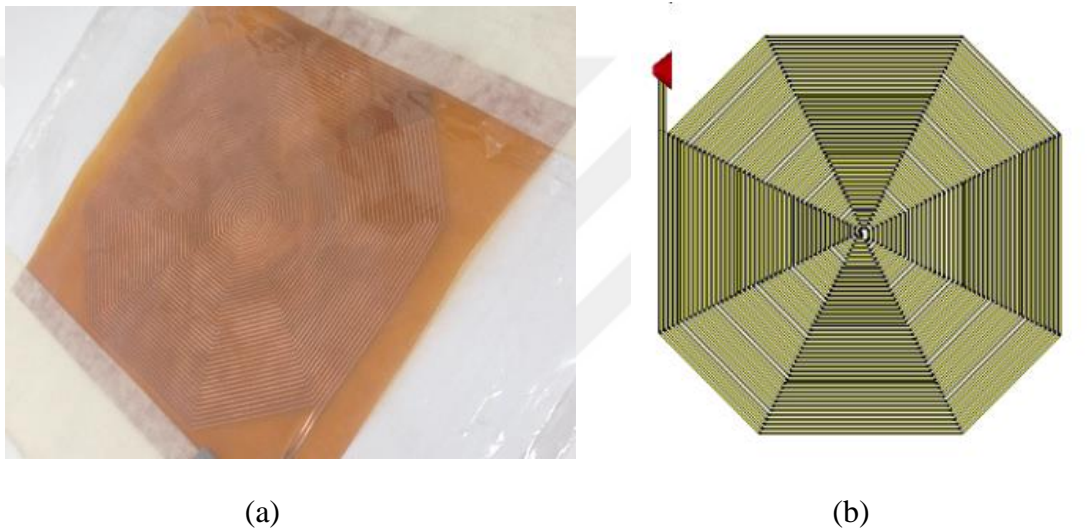


Figure 3.6: (a) Flexible Kapton Antenna at 27 MHz (b) Antenna prototype at CST Studio.

3.3.2 Impedance Matching

In electronics, impedance matching is the practice of designing the input impedance of an electrical load or the output impedance of its corresponding signal source to maximize the power transfer or minimize signal reflection from the load. Impedance matching is a fundamental aspect of RF design and testing; the signal reflections caused by mismatched impedances can lead to serious problems.

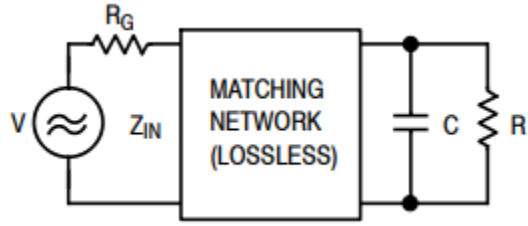


Figure 3.7: General Matching Conditions.

In generally, matching network design requires a trade off between bandwidth, complexity, implementation, adjustability for desirable attributes. For these requirements, the input impedance is usually 50Ω (Figure 3.8).

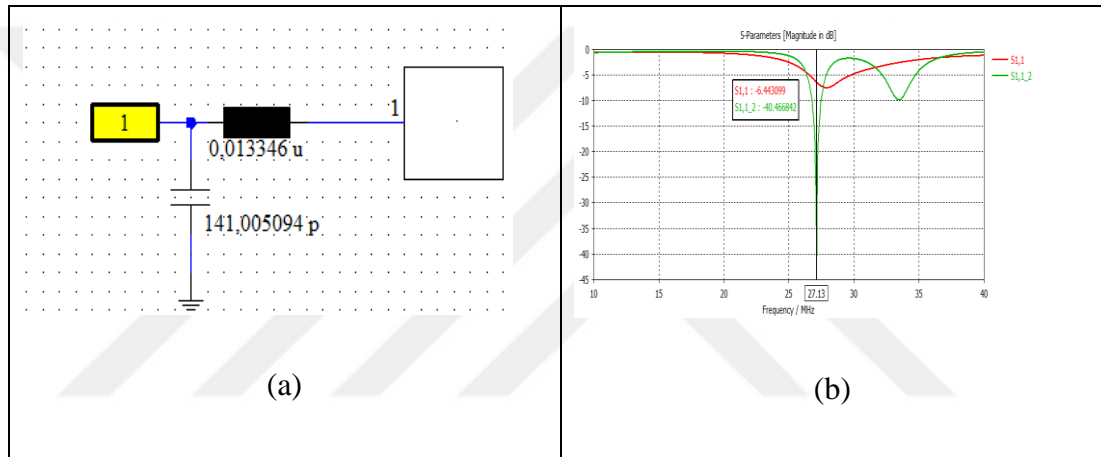


Figure 3.8: (a) Antenna matching at CST Studio (b) Antenna of S11 matching and non-matching form.

3.4 Results and Discussion

Selected antennas, coil and Helmholtz coil for project were compared with CST Studio. E Field and H Field values of PEMF system and antennas are determined as shown in the picture. System block diagrams have been prepared accordingly systems have been established.

3.4.1 Simulations and Measurements of Pulsed Electromagnetic Field (PEMF)

When the various studies in the literature are examined, the parameters that are important for the experiments are exposure time, frequency, waveform and the

intensity of the electromagnetic field. Considering these parameters, CST Studio simulations are most effective in comparing the distance between the coils and the different results in different coils. The homogeneous density in the center of the coil, the E Field and H Field values falling as they move away from the antenna are the best examples of this. Tissue samples were added to these simulations in a petri dish and simulations were made more valuable.

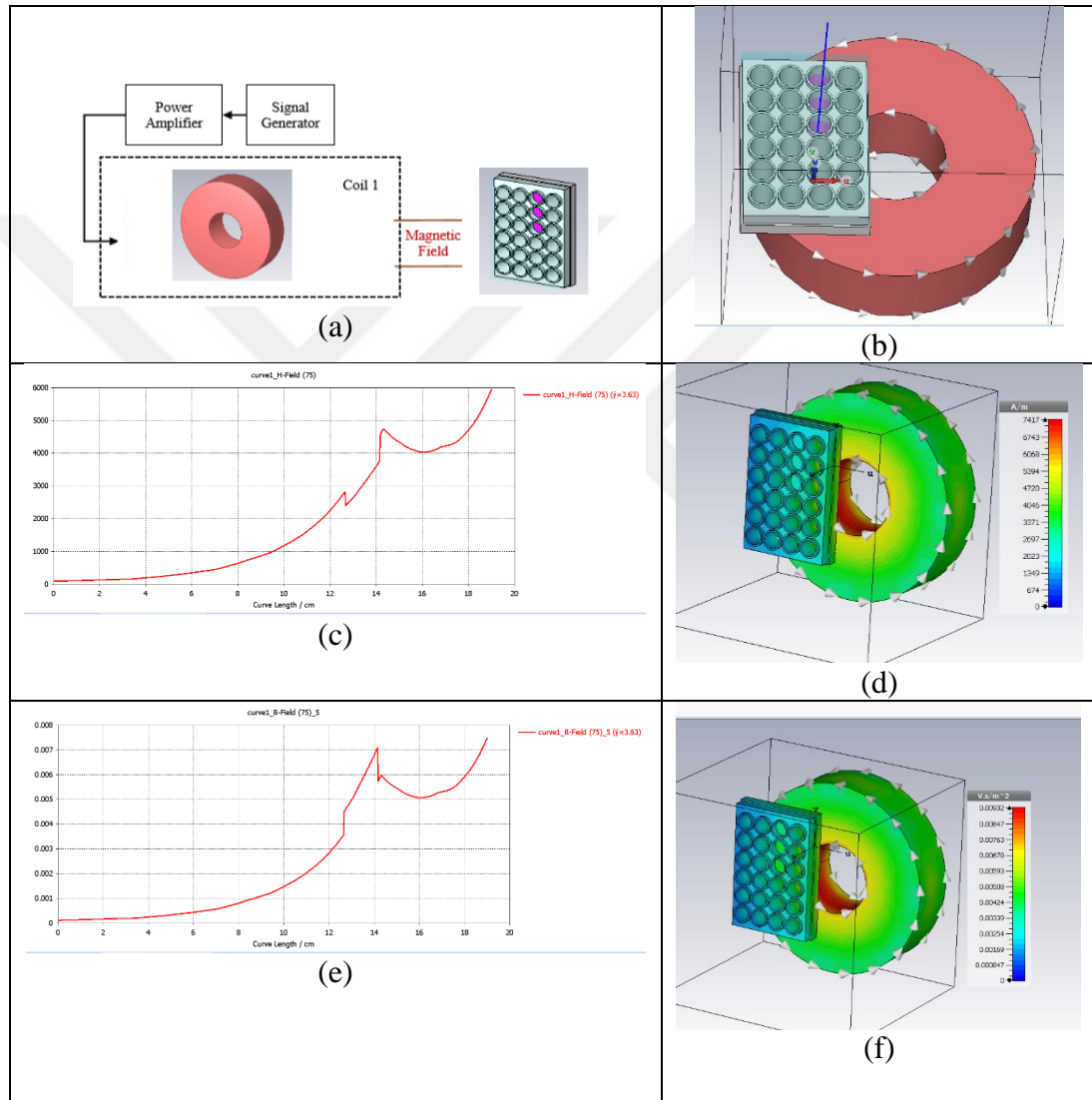


Figure 3.9 : (a)PEMF system block diagram with petri dish (b) Designed coil with petri dish (c) H- Field on curve along coil to petri dish (d) H field distribution on PEMF system (e) E- Field on curve along coil to petri dish (f) E field distribution on PEMF system.

These simulations gave information about E Field and H Field values to be exposed to the system (Figure 3.9) . Simulations were made for two separate PEMF devices.

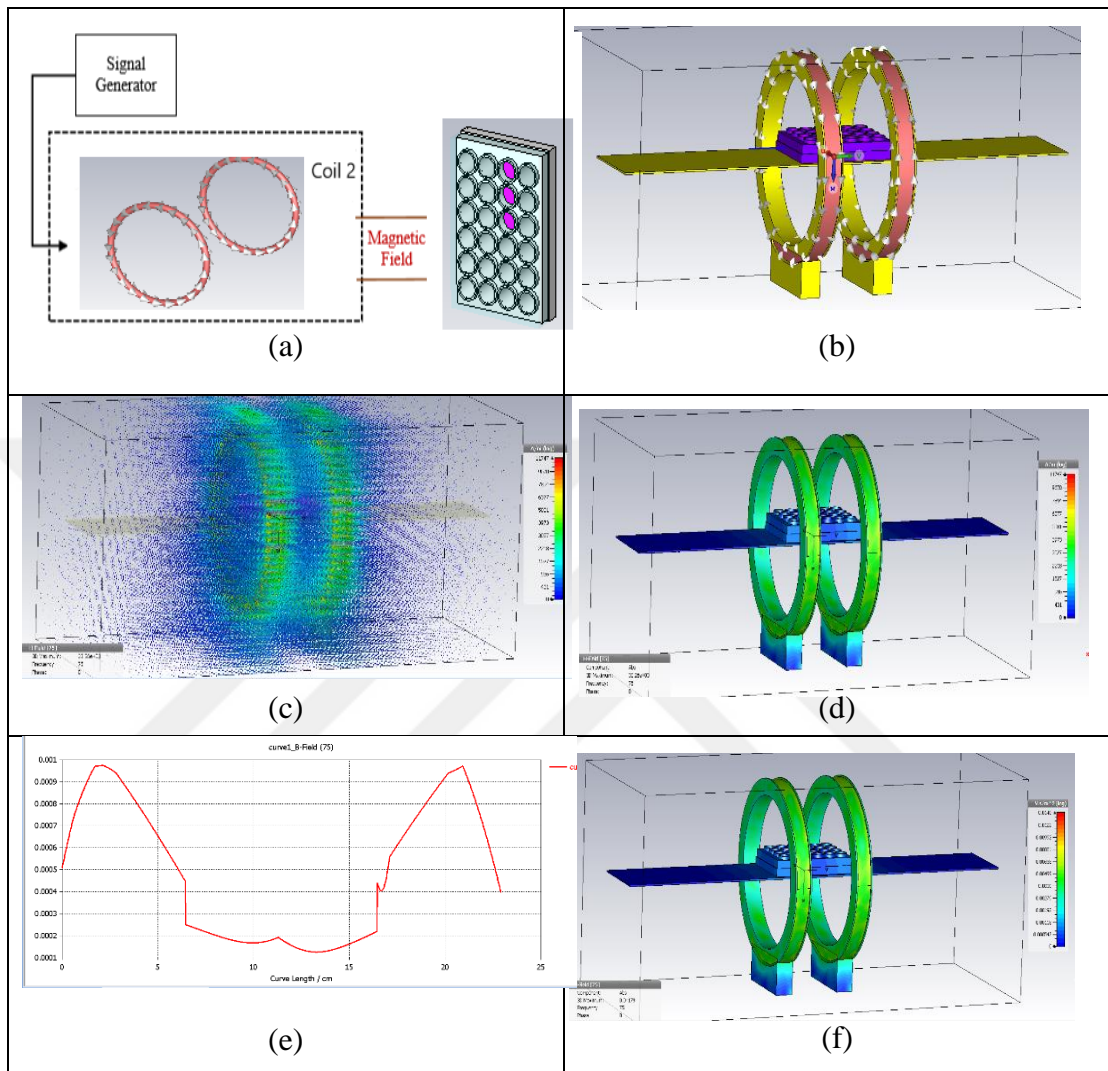


Figure 3.10 : (a) Helmholtz coil PEMF system block diagram with petri dish (b) Helmholtz coil with petri dish (c) H- Field simulation of the system (d) H field distribution on Helmholtz coil PEMF system (e) E- Field on curve along coil to petri dish (f) E field distribution on Helmholtz coil PEMF system.

3.4.2 PRFE Antenna Simulations and Measurement Results

Microstrip patch antenna that is designed and manufactured as the basis for use in PRFE therapy. First, in the basic design, an antenna modeled on the FR4 dielectric material substrate $h = 1.6$ mm thick is designed. In this design, the dimensions are 120 mm x 120 mm x 1.6 mm and have 14 turn numbers with a thickness of 2.2 mm.

Designed for 27 MHz, this antenna was then added with an appropriate impedance matching to improve its efficiency. The simulation results are as shown in the figure (Figure 3.11).

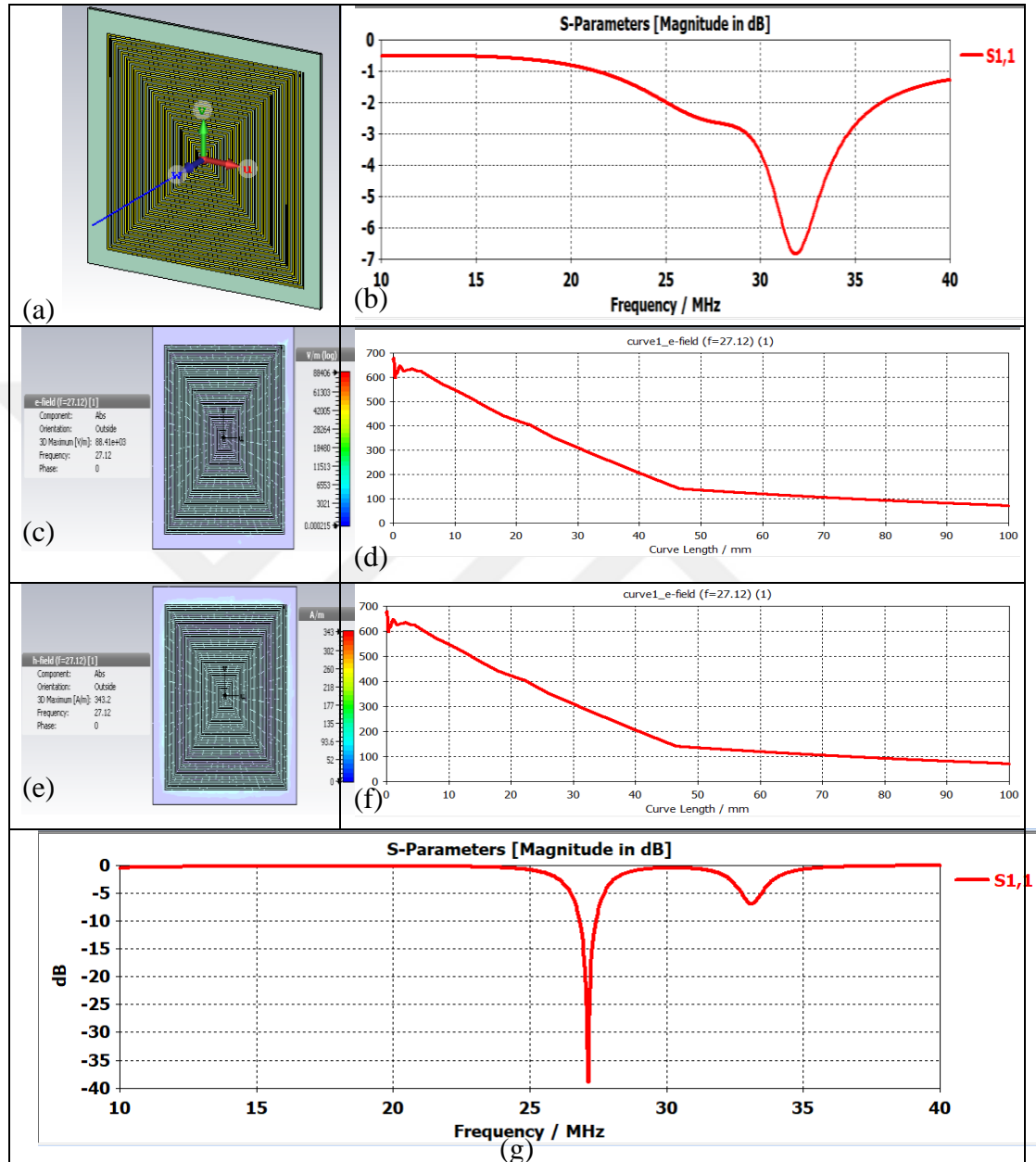


Figure 3.11: Simulation results of the designed antenna at 27.12 MHz (a) Front view of antenna (b) Simulation results of antenna without matching (c) E-field simulation result (d) E-field result through 10 cm line from the antenna (e) H-field simulation result (f) H-field result through 10 cm line from the antenna (g) Simulation result of antenna with matching.

4. PEMF AND PRFE EXPOSURE SYSTEM DESIGN, MEASUREMENTS

4.1 Overview

PEMF and PRFE exposure system is detailed in Chapter 4. In this section, the mechanisms of PEMF system is presented with used amplifier and waveforms. In the same way, the PRFE system is described in detail with system equipment amplifier. L929 fibroblast cells exposed in these designed devices allowed us to obtain significant results after the experiment. Experiments were performed simultaneously in the same medium. In the PEMF system exposed cell lines in and the PRFE system exposed cell lines in were equal conditions at the same room temperature in the same environment.

4.2 PEMF Experimental Setup

At the beginning of the project, experimental investigations were carried out on the coils selected from the literature and used Pasco Helmholtz coil and designed coil. We have designed this mechanism in two different ways to observe the effects of wound healing on L929 fibroblast cell line with magnetic field and temperature sensors. In the first system, the system designed with Kikusui Bipolar Power Supply device fed with Class D-Amplifier with 75 Hz square wave is used. In the other system, Pasco Helmholtz coils fed by Pasco Function Generator at 75 Hz.

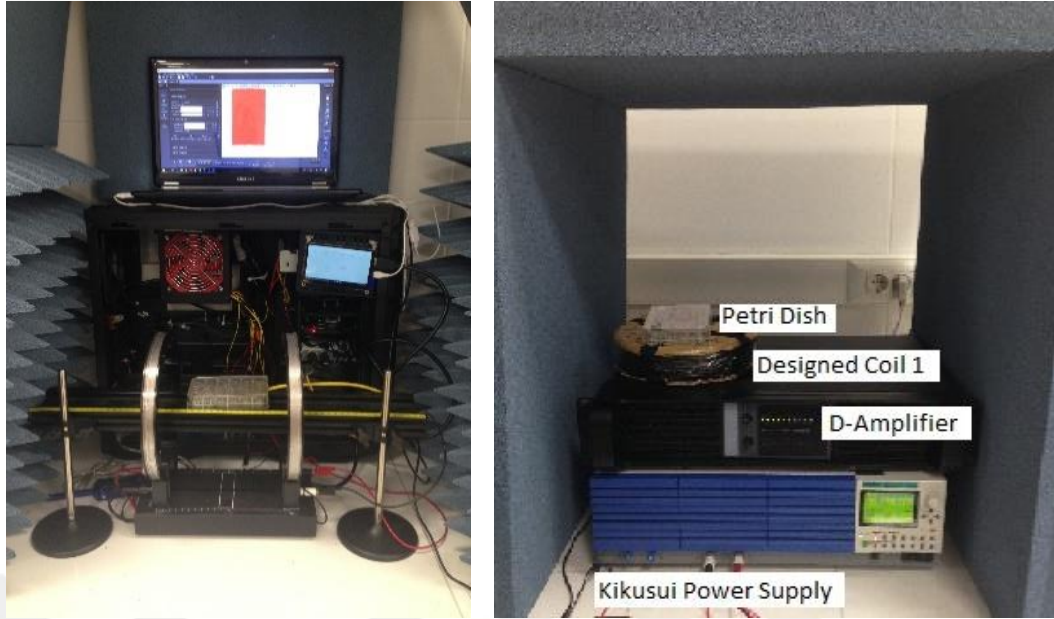


Figure 4.1: Laboratory equipments used in the project.

Laboratory equipments used in the project are as follows (Figure 4.1)

- Pasco Helmholtz Coil
- Kikusui bipolar power supply
- FP14000 Class -D Amplifier
- Pasco Magnetic Field sensor
- Pasco Function Generator,
- Arduino Microprocessor
- LattePanda Microprocessor and touch screen

Magnetic field and temperature sensors, In order to explain the experimental mechanisms in which the cell culture is exposed to the electromagnetic field;

- i) PEMF exposure system is used to generate the uniform time-varying electromagnetic fields with Kikusui Bipolar Power Supply with magnetic induction (magnetic flux density) up to 4 mT (Figure. 4.2).

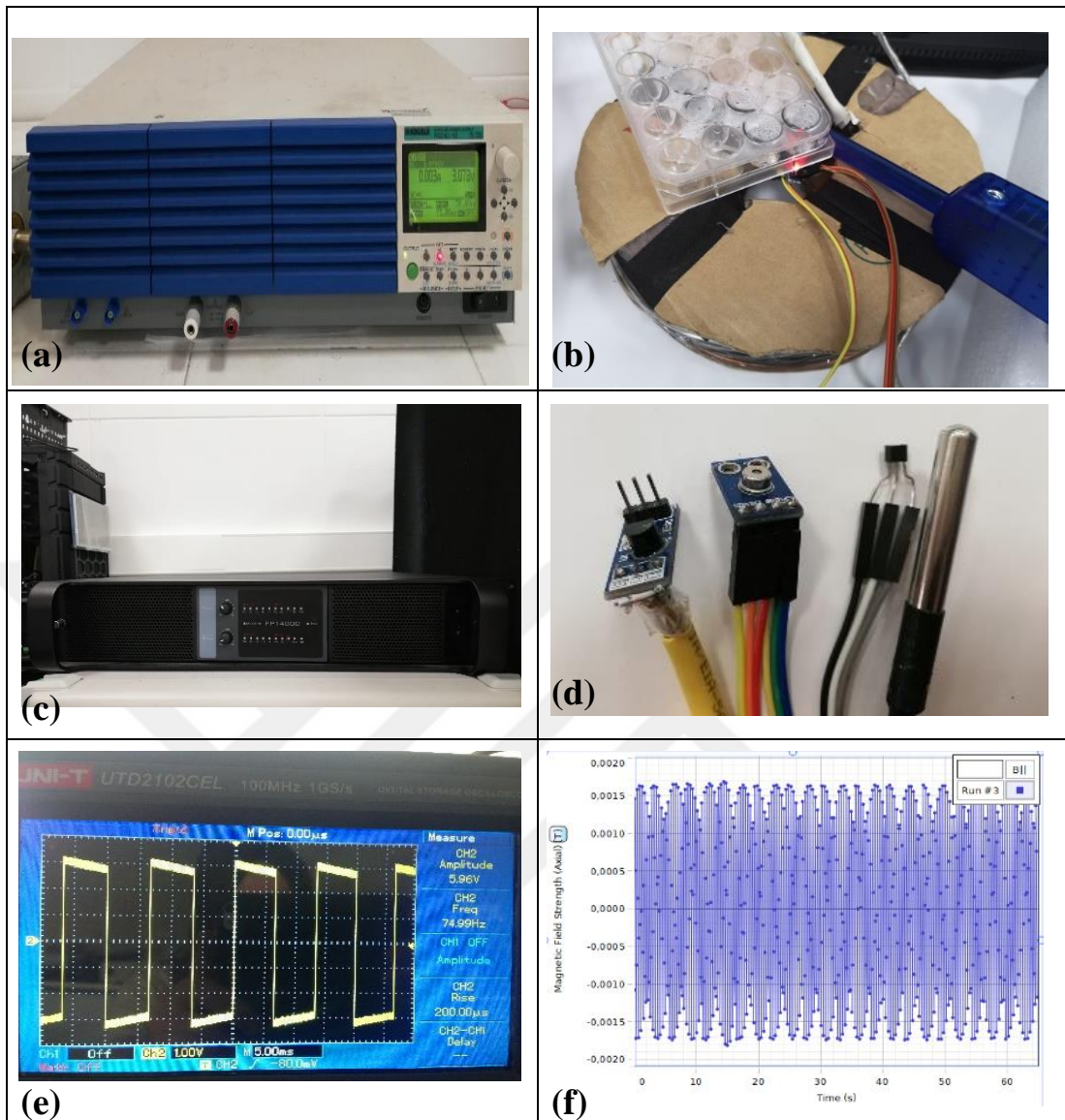


Figure 4.2 : PEMF exposure system with designed coil (a) Kikusui Power Generator (b) Exposure of the cell culture to the electromagnetic field (c) FP14000 Class -D Amplifier (d) Arduino sensors (e) Real-time signal display at 75 Hz (f) Measured with Pasco Magnetic Sensor B-Field value at mT.

ii) PEMF exposure system with Pasco Helmholtz coil is used to generate the uniform time-varying electromagnetic fields with Pasco Function Generator with magnetic induction (magnetic flux density) up to 1 mT (Figure 4.3).

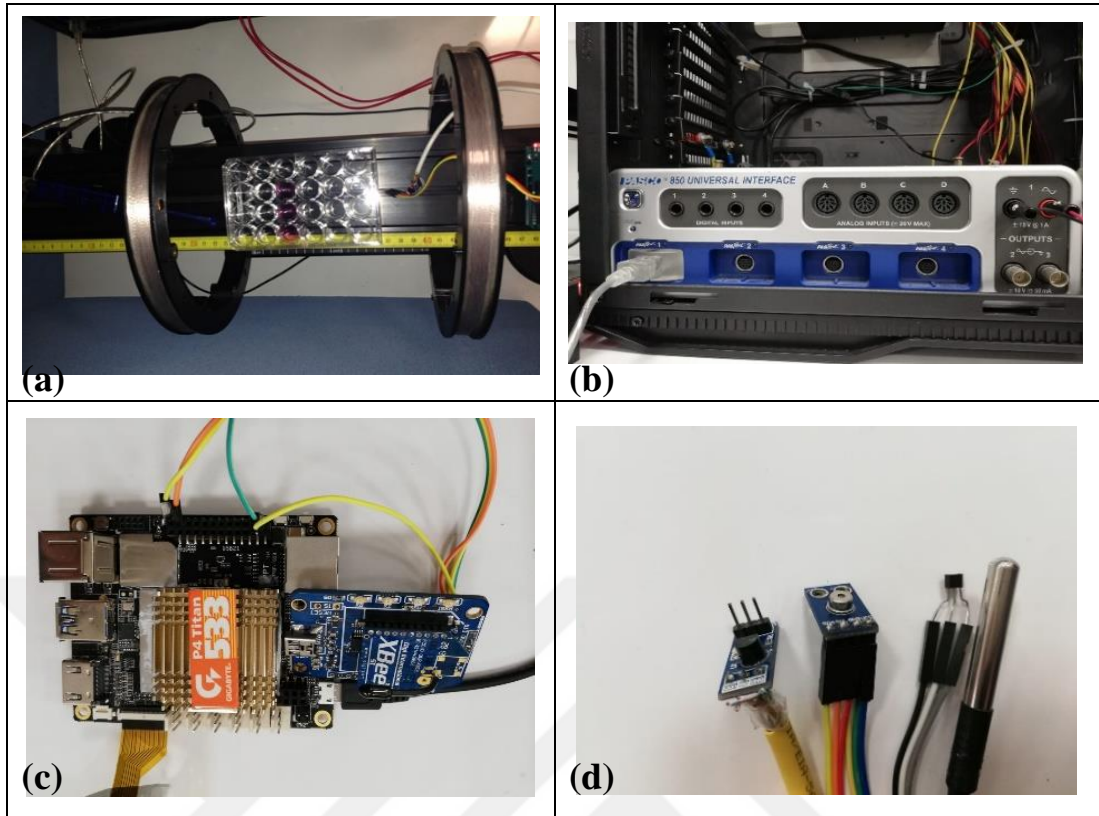


Figure 4.3: PEMF exposure System with L929 fibroblast cell line (a) Pasco Helmholtz Coils with sensors (b) Pasco Function Generator (c) LattePanda Display showing sample data received from sensor (d) Arduino system with sensors.

4.2.1 PEMF Waveforms

Systems using various waveforms such as sine, triangle, trapezoidal or time-varying waveforms do not fully meet the pulsed waveform. The pulsed electromagnetic field must have an instant rise time to form the impact form. In this way, magnetic field intensity may be instantaneous. Continuing waves in this cycle create expanding magnetic fields, and then the signal intensity decreases again to zero.

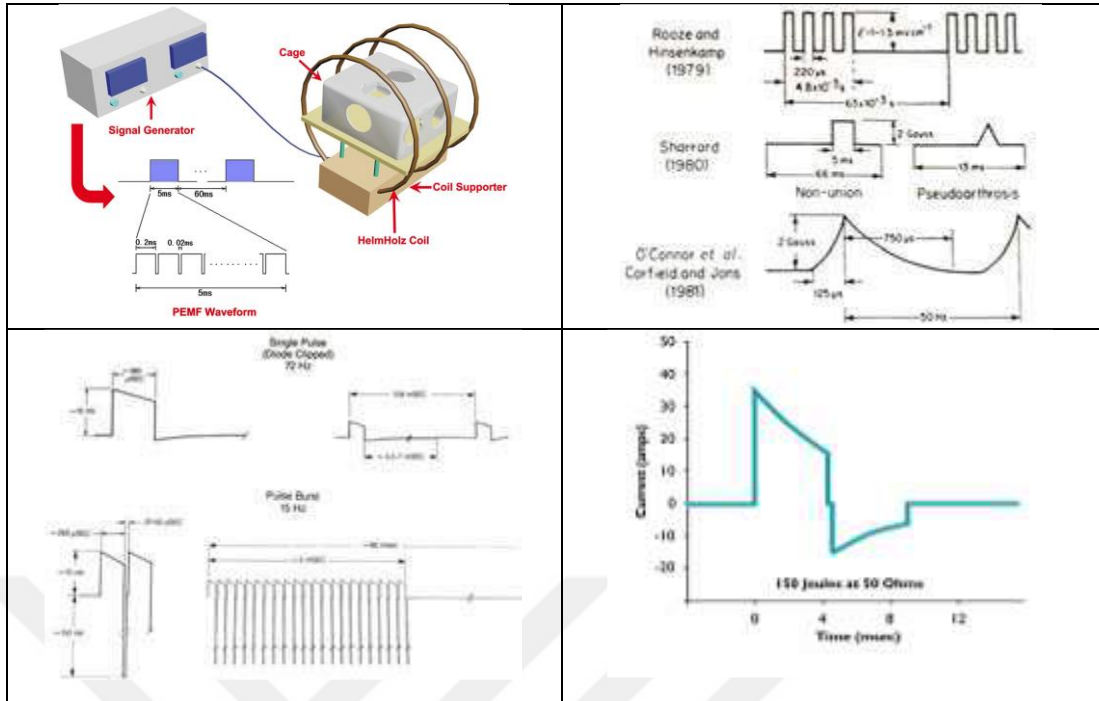


Figure 4.4: Some of the PEMF / PRFE waveforms in the literature.

4.3 Class D Amplifier for PEMF System

Class D power amplifiers are a type of amplifier that contains mosfets, which can be operated as binary switching functions (Figure 4.5). While the mosfets operate smoothly as binary switching, there is no time difference between the transition of the circuit stages and no loss of power in the zero input condition. The signal to be amplified is in the form of a series of fixed amplitude pulses, and the active devices move rapidly back and forth between completely conductive and non-conductive states. When the ideal binary switching is in the transmission state, it passes all currents even though the voltage is not induced. Switching is triggered on the whole voltage when it is cut and no current flows inside. In this circuit, the power is not wasted on the switching elements that provide this strength, and these results in incredible power values because of power in the class D power amplifiers.

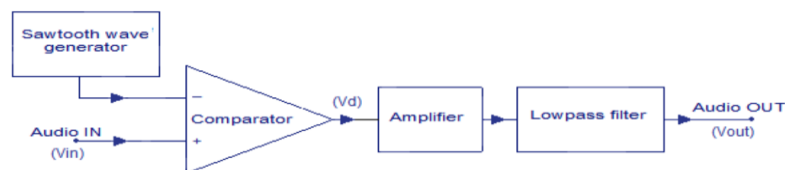


Figure 4.5: Class D Power Amplifier block diagram.



Figure 4.6: FP14000 Class TD Profesyonel PA Power Amplifier.

4.4 Active PRFE Experimental Setup

At the beginning of the project, PRFE systems and antenna applicators were investigated. In the later stages, some modifications to the antenna applicators were made and the performance of the applicators were improved. PRFE exposure system with PSK signal modulation is used to generate uniform time-varying magnetic fields at 27.12 MHz. We have designed this mechanism observe the effects of wound healing on L929 fibroblast cell line with magnetic field and temperature sensors.

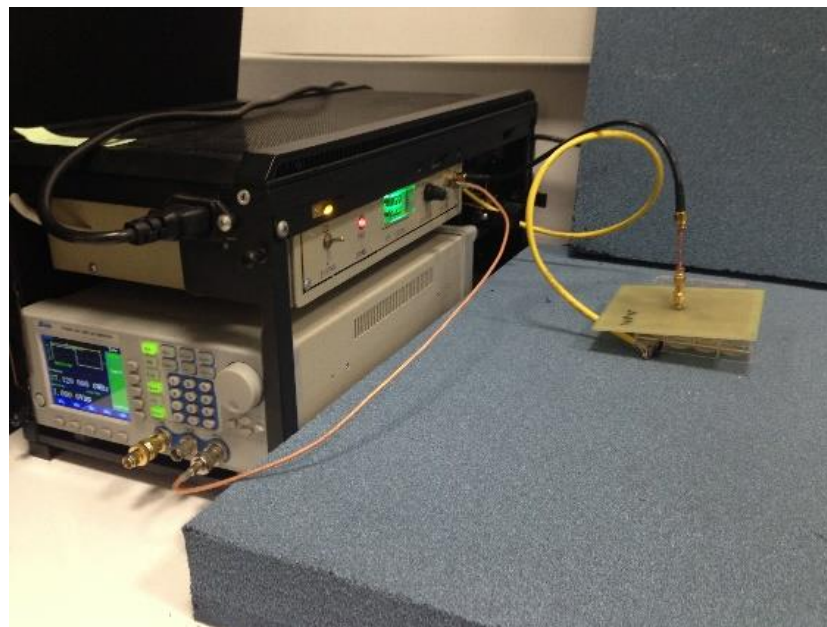


Figure 4.7: Laboratory equipments used in PRFE exposure system.

Laboratory used in the implementation of the project equipments (Figure 4.7):

- Sui function Waveform Generator
- Power Amplifier
- Antenna applicator
- Arduino Microprocessor
- LattePanda Microprocessor and touch screen
- Magnetic field and temperature sensors

The cell line was exposed to PRFE for 4 hours. The system consists of a square patch applicator antenna with a length of 12 cm. The cell line was exposed to 7 mT produced by the antenna applicator. The cell line was placed at the center of the antenna where the magnetic field was at its highest center point (Figure 4.8).

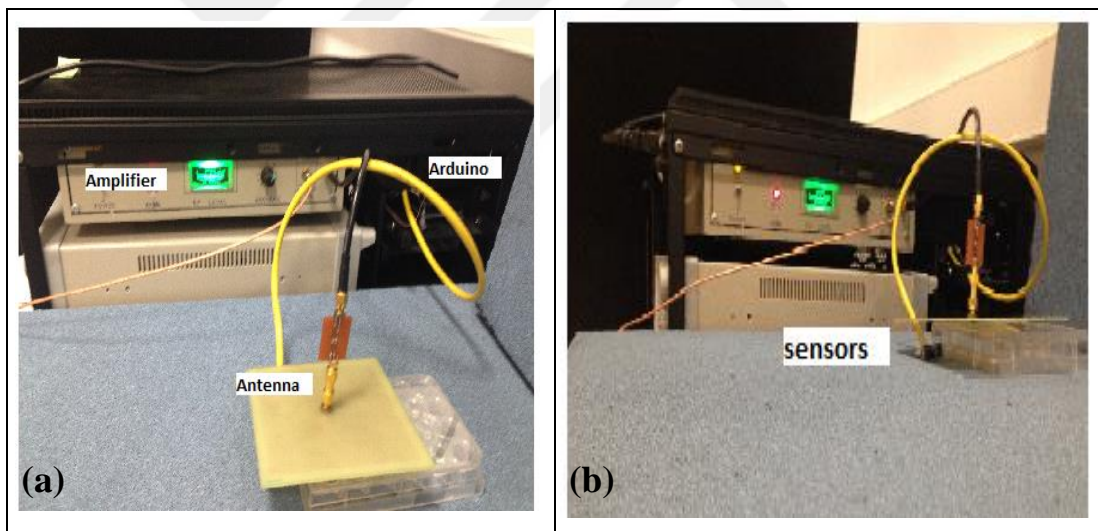


Figure 4.8: (a) PRFE exposure system (b) Position of the sensors during the experiment.

4.4.1 Fabrication of Antenna Prototype

Before the antennas we designed, we took the measurements of the B field and the H field values in the CST Studio. Then we produced the antennas and we measured the antennas to see if they matched the simulation values. We used the Signal Hound EMC

E5 E-Field probe and the H-Field probe with the Anritsu Spectrum Analyzer (Figure 4.9).

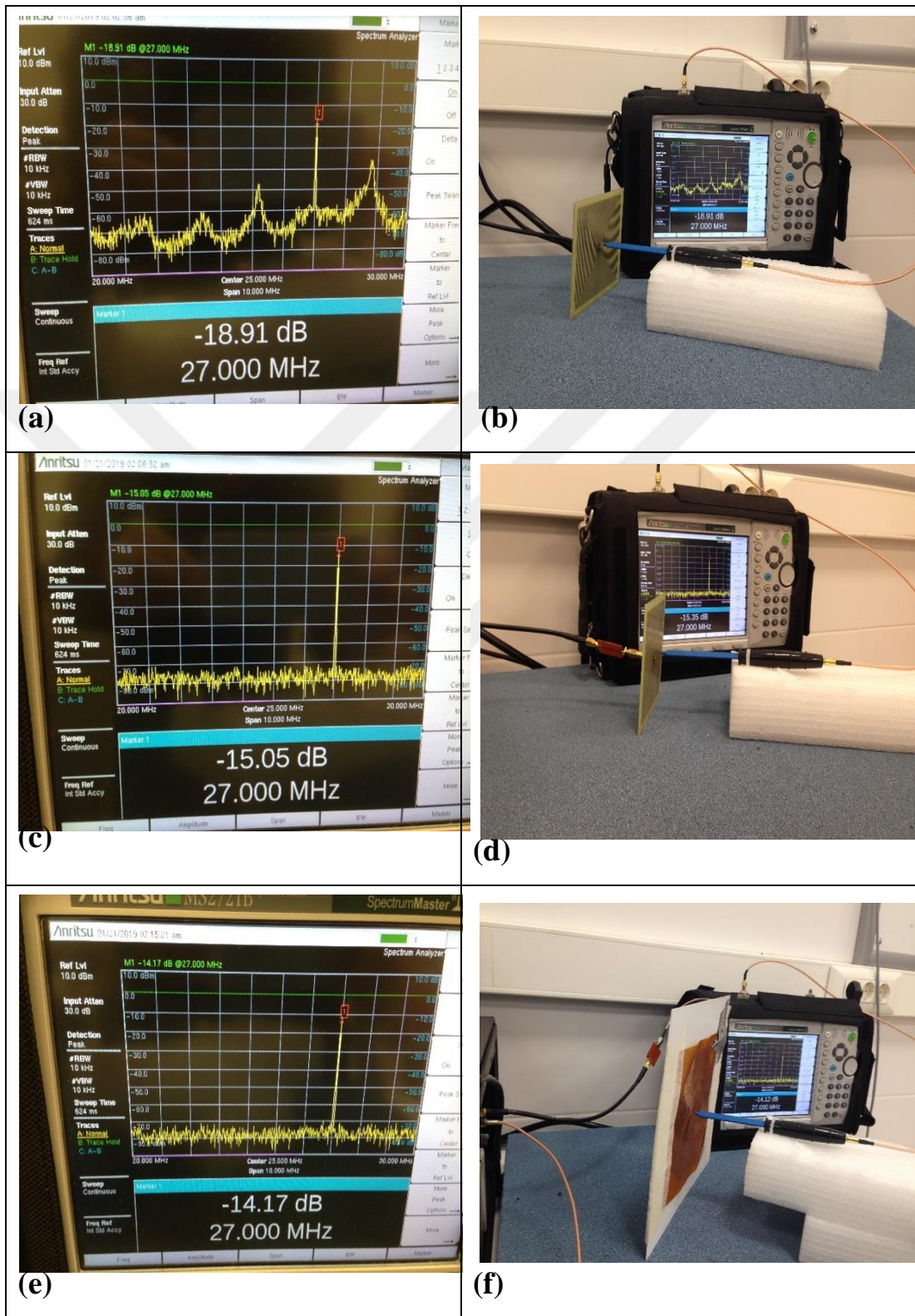


Figure 4.9 : (a) FR-4 antenna E-field -18.9 dBm (b) Antenna measurement system with Signal Hound EMC E5 E-Field probe (c) FR-4 matching antenna E-field -15 dBm (d) Antenna measurement system with Signal Hound EMC E5 E-Field probe (e) Kapton matching antenna E-field -14 dBm (f) Antenna measurement system with Signal Hound EMC E5 E-Field probe.

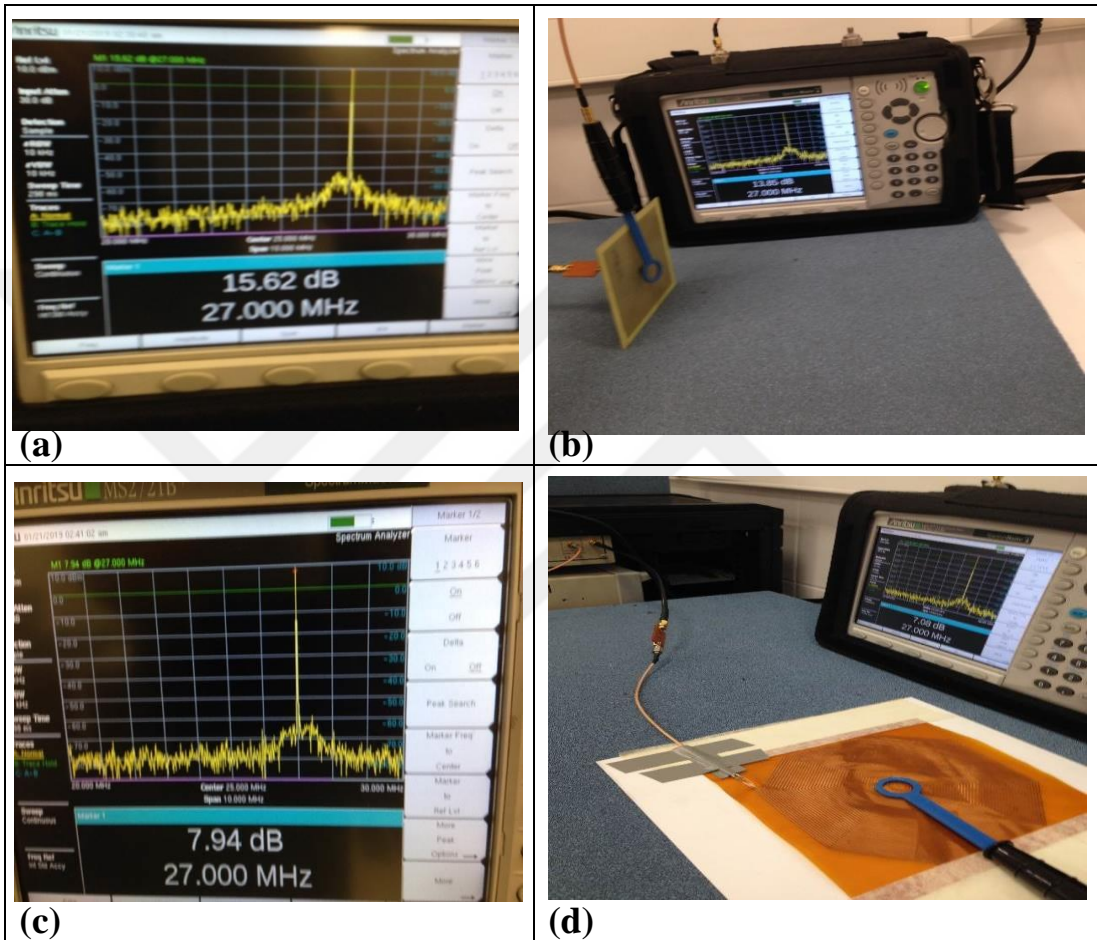


Figure 4.10 : (a) FR-4 antenna H-field 15 dBm (b) Antenna measurement system with Signal Hound EMC H20 H-Field probe (c) Kapton antenna H-field 8 dBm (d) Antenna measurement system with Signal Hound EMC H20 H-Field probe.

5. WIRELESS SENSOR NETWORK APPLICATIONS FOR PEMF / PRFE

5.1 Material and Methods

Wireless Sensor Networks are the combination of embedded system and wireless communication that allows data transmission among the sensor nodes over wireless networks. The system provides a user interface for any user to access the current and past sensor readings in different rooms. The diagram of the system is shown in Figure 1 and consists of a LattePanda that provides an interface to the system, a coordinator as a data collector and web server, and several end devices that provide sensor readings over Xbee communication links.

5.2 Wireless Sensor Network Experimental Setup

This paper presents a wireless sensor network (WSN) prototype system for temperature and magnetic field monitoring in tissue during the experiment. The DS18B20 and the MLX90614 for the temperature sensors, the PASCO magnetic field meter for the magnetic field and the DRV5053 Analog-Bipolar Hall Effect sensor were used.. The data was obtained from the sensor program by the interface program. Arduino-based wireless data transfer was designed with XBee S1.

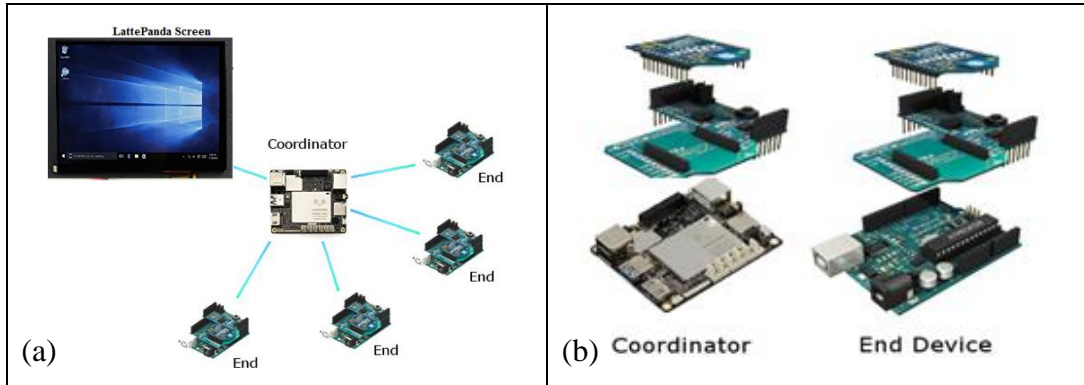


Figure 5.1: (a) System Diagram (b) Arduino -Lattepanda connection and Arduino-Xbee connection for end device of the wireless network system.

Table 5.1: Specifications of sytem equipments.

Sensor or equipment	Model	Accuracy
Digital Temperature Sensor	DS18B20	$\pm 0.5^{\circ} \text{C}$
Analogue Temperature Sensor	LM35	$\pm 1^{\circ} \text{C}$
Infrared Temperature Sensor	MLX90615	$\pm 0.5^{\circ} \text{C}$
Magnetic Field Sensor	DRV5053	
Aurdino	UNO-MEGA	
LattePanda	LattePanda	
Wireless Shield	XBee Shield	
Xbee	S1	
LattePanda Touch Screen	7" IPS Display	

5.2.1 Wireless Sensor Network Using with Xbee

Wireless Sensor Network system consists of two main elements: XBee and Arduino. We use the XBee S1 802.15.4 low-power module wire antenna modules based on the IEEE 802.15.4/Zigbee Wireless Personal Area Network (WPAN) standards to build a low-power, low maintenance, and self-organizing Wireless Sensor Network [1]. The reason for choosing Xbee for this project; Simple, out-of-the-box RF communications, no configuration needed Point-to-multipoint network topology 2.4 GHz for worldwide deployment – Common Digi XBee footprint for a variety of RF modules – Low-power sleep modes – Multiple antenna options[3]. The network consists of a data gateway or coordinator that wirelessly polls each WSN sensors-monitoring node located in each

experiment. The Coordinator is the center of system. It collects sensor readings from the sensors back to the system. The incoming datas are displayed and saved in the interface on the screen of LattePanda.

In this project, we use Arduino different variations like Arduino UNO, Arduino Mega 2560, Arduino Leonardo.

XBee is a wireless communication module that Digi built to the 802.15.4/ZigBee standard. The ZigBee wireless standard can form self-healing mesh networks. XBee and XBee-PRO 802.15.4 OEM RF modules are embedded solutions providing wireless end-point connectivity to devices. These modules use the IEEE 802.15.4 networking protocol for fast point-to-multipoint or peer-to-peer networking. They are designed for high-throughput applications requiring low latency and predictable communication timing. XBee modules are ideal for low power, low-cost applications. XBee-PRO modules are power-amplified versions of XBee modules for extended-range applications.

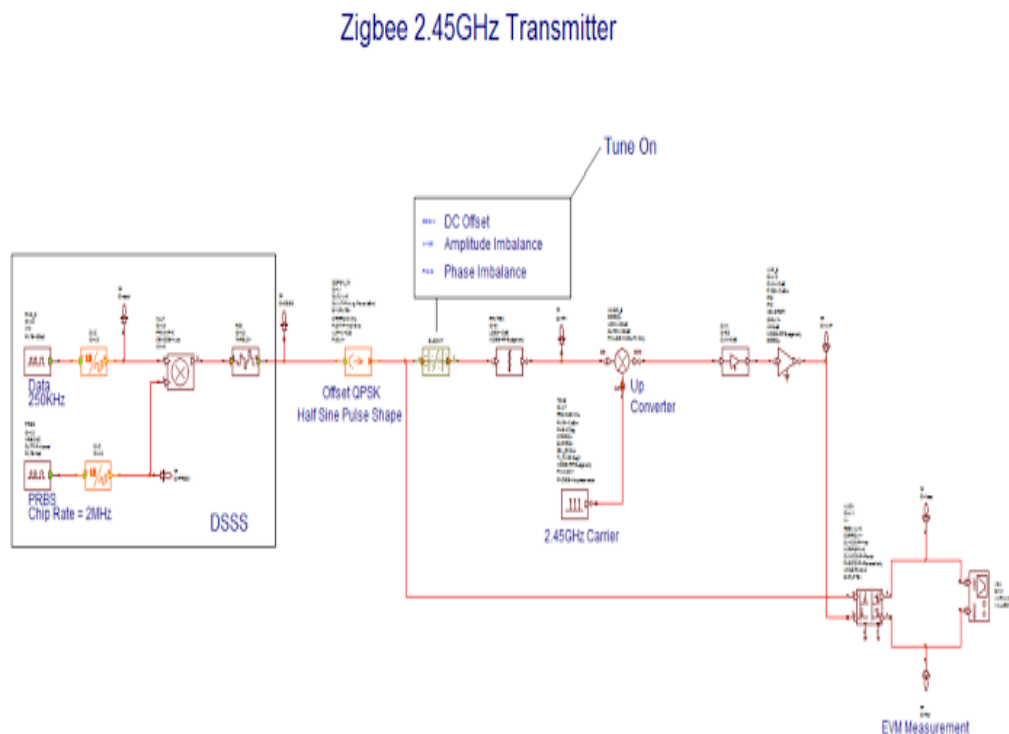


Figure 5.2 : Zigbee System Diagram at 2.45 GHz.

ZigBee was simulated to see how the operation. Using fort his AWR Version 9.01. At 2.45 GHz ZigBee transmitter that has the same functionality as thesystem directly below (Figure 4.9). It also shows how to introduce amplitude imbalance, phase imbalance, and DC-offset to the TX signal through use of the "Input Imbalance" subcircuit, which can be found in the Elements tree under System Blocks/Libraries/RF Blocks. When the simulation is running, an EVM measurement is performed as you tune on DC-offset, Amplitude Imbalance, and Phase Imbalance.

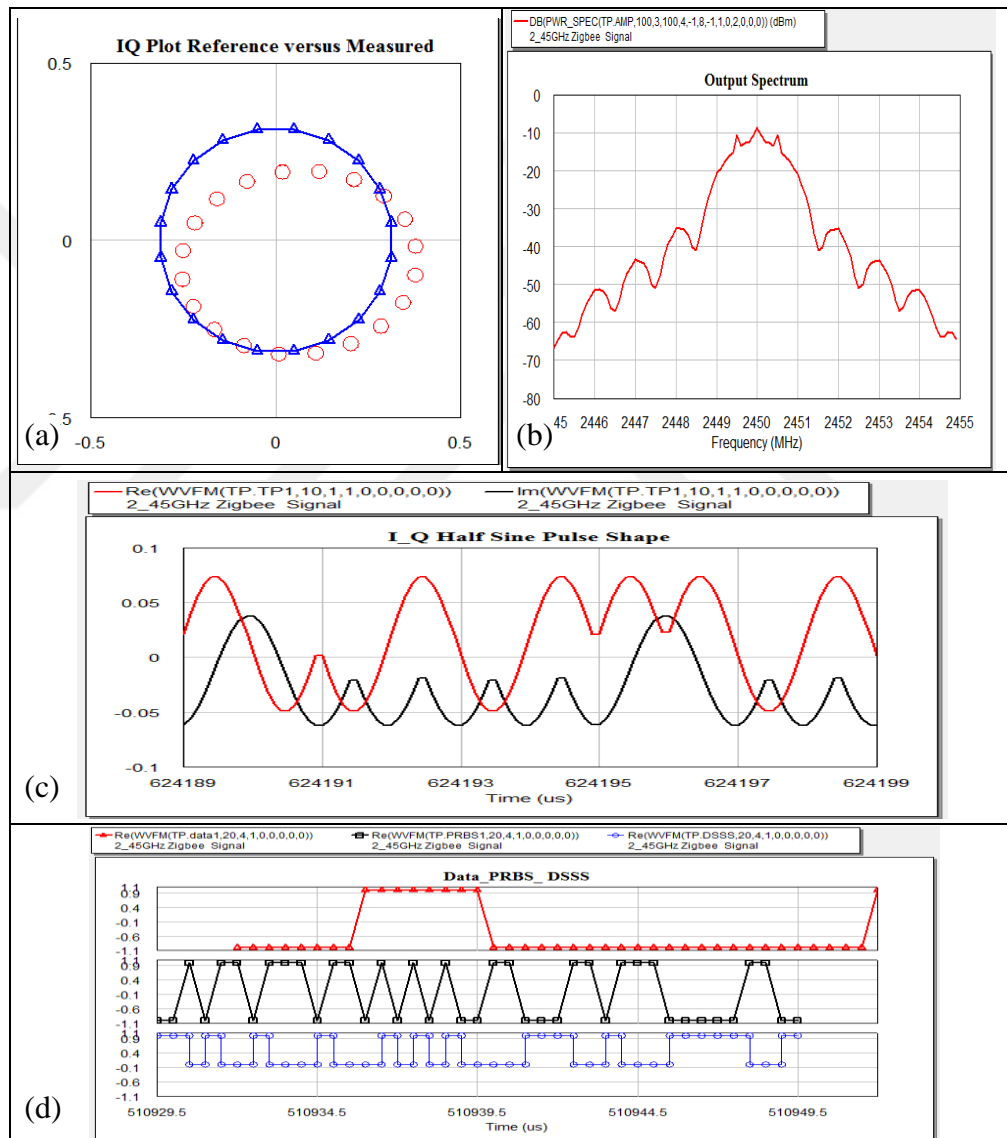


Figure 5.3 : After this simulation we can take the dates graphic about (a) IQ Plot Reference versus Measured (b) Output Spectrum (c) I_Q Half Sine Pulse Shape (d)Data- PRBS- DSSS.

5.2.2 Arduino with Pulsed With Modulation

Arduino is an open-source micro-controller system which has a small chip for computational work and memory storage. Arduino is used for creating a prototype as well as to develop standalone interactive objects [30]. Arduino uses the USB connector to upload code or for a power connection. The board can work on 7V to 12V. Arduino was developed with requirements as easy to learn and use, flexible, reliable. They are widely used in a wireless sensor network as a portable device [31]. In this project, we use Arduino different variations like Arduino UNO, Arduino Mega 2560 , Arduino Leonardo.

Arduino Uno can communicate in many ways which is used in this project. Serial communication is possible with RX and TX pins. Therefore, it provides ease of use in projects. The features of Arduino UNO used in the project are as follows; ATmega328 was used as microcontroller. There are 14 digital input / output pins and 6 analog pins on it. The input voltage is 7-12V, the output voltage is 6-20V and the operating voltage is 5 V. The DC Current per input / output pin is 40 mA and the DC Current for 3.3V input is 50 mA. Its small dimensions allow for ease of positioning compared to other Arduino variants. Its length is 68.6 mm and its width is 53.4 mm.

To explain it simply, Pulsed Width Modulation is a technique used to adjust the width of the generated pulses. PWM technology, changing the width of the generated square wave signal is based on. Square wave signals, such as we see on the side, and from 0 to 1 occurs (1 = 5V, 0 = 0V). It is equal to the width of two normal conditions. However, when applied to the PWM technique '1' it means here '5V' pulse width can be changed. Using PWM methods on arduino basic reasons are; analog results from digital results can be obtained with PWM technique, square wave allows the production. For communication to "0" and "1" s in the logic circuit comprising a square wave and PWM communications are used.

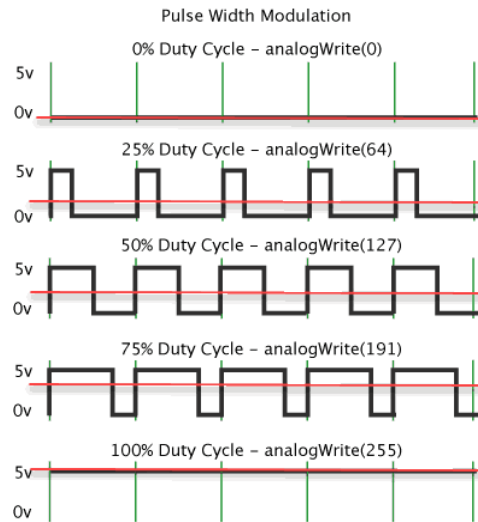


Figure 5.4: Pulsed with modulation.

5.3 Hall Effect Sensor and Measurements

Hall Effect Sensors consist basically of a thin piece of rectangular p-type semiconductor material passing a continuous current through itself (Figure 5.5). When the device is placed within a magnetic field, the magnetic flux lines exert a force on the semiconductor material, which deflects the charge carriers, electrons and holes, to either side of the semiconductor slab. This movement of charge carriers is a result of the magnetic force they experience passing through the semiconductor material [32]. In this project we use DRV5053 Analog bipolar Hall Effect sensor which is of the chopper-stabilized Hall IC that offers a magnetic sensing solution with superior sensitivity stability over temperature and integrated protection features [33].



Figure 5.5 : DRV5053 Analog-Bipolar Hall Effect Sensor.

5.4 Temperature Sensors and Measurements

The DS18B20 provides 9 to 12-bit (configurable) temperature readings which indicate the temperature of the device (Table 5.2). The DS18B20 communicates over a 1-Wire bus so that only one wire (and ground) needs to be connected from a central microprocessor.

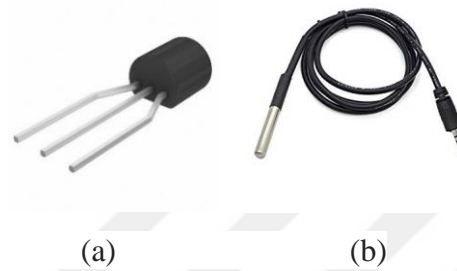


Figure 5.6: (a) (b) DS18B20 Waterproof Temperature Sensor.

Two types are available, one of them is consisting of a waterproof probe and long wire shape, which is perfect for immersive temperature detection detecting something far away (Figure 5.6).

Table 5.2 : Specifications of DS18B20 Temperature Sensor.

Parameter	Specification
Temperature Range	-55 °C to +125 °C (-670 F to +2570 F)
Resolution	9-12 bit
Accuracy	±0.5 °C (-10 °C – +85°C)
Power Usage	3V to 5.5V

In order to describe the Arduino based system we used during the experiment, it consists of two temperature sensors and one Hall Effect sensor. The connection type of the sensors used is as shown (Figure 5.7).

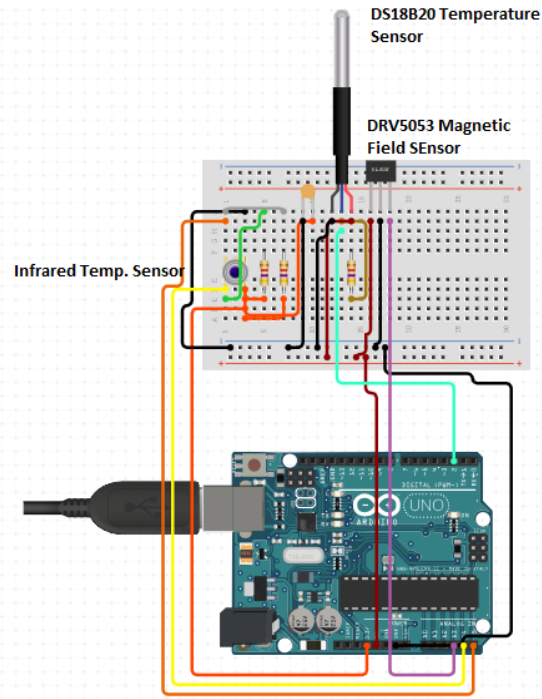


Figure 5.7: Connection with Arduino in the Sensor Network.

5.5 E-Health Sensor With in PEMF System

The e-Health Sensor Shield allows performing medical applications where body monitoring is needed by using different sensors with Arduino. Sensor datas gathered can be wirelessly sent using with XBee. This platform allows you to collect many sensor data during the experiment.



Figure 5.8: E-Health Sensor Kit.

It can use as many sensors such as pulse, oxygen in the blood (SPO2), airflow, body temperature, galvanic skin response, blood pressure, patient position, ECG etc (Figure 5.8).

5.6 Interface Display with Lattepanda

LattePanda is an easy to use, advanced microprocessor with Windows 10 operating system that is embedded on Arduino (Figure 5.9). The hardware features of the device are:

- Intel Atom 4-Core 1.84GHz processor
- 500Mhz Graphics processor
- 4 GB DDRL3L RAM
- 64GB EMMC Memory
- WiFi and Bluetooth 4.0
- 2x USB 2.0
- 1x USB 3.0
- HDMI Output
- Display & Touch connectors
- Audio output
- MicroSD card slot
- Ethernet connection
- Arduino microcontroller
- Arduino pins and 6x 3-pin connector connectors
- Direct I2C and UART connection to the processor

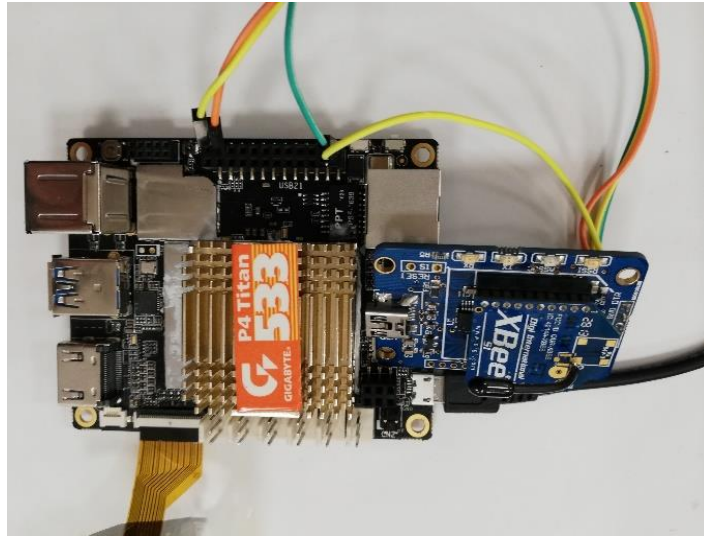


Figure 5.9 : LattePanda with XBee.

Thanks to these features, it is working as a portable computer with the touch screen it is connected to and it is used as interface peer in this project. With the XBee shield we have mounted on it, it has easily become part of the wireless sensor system. It is the receiver of the sensor data in the project and displays them in the interface program.

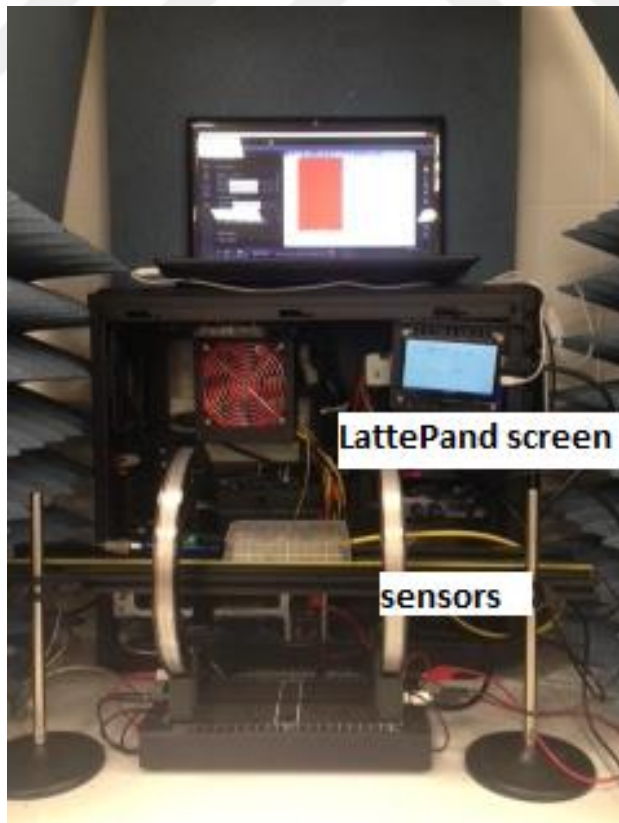


Figure 5.10 : PEMF exposure system with LattePanda

Arduino-based system receives the data received by sensors. During the experiment, the interface program instantly records the received data as shown (Figure 5.10).

5.6.1 Interface Program for Sensor Applications

Displaying the data received from the sensors on the Arduino interface allows only read the data. One of the most important things during an experiment is the evaluation of the received data. It is important to record and chart these data. The interface platform, display two columns of data, magnetic field and temperature (Figure 5.11). The background database is the foundation and core of the system, which is used for recording sensors data. The platform provides sketching the graph of the data and converts to excel and Matlab files. This interface program embedded in the Latte Panda allows the system to easily retrieve, store and convert data without the need for a computer.

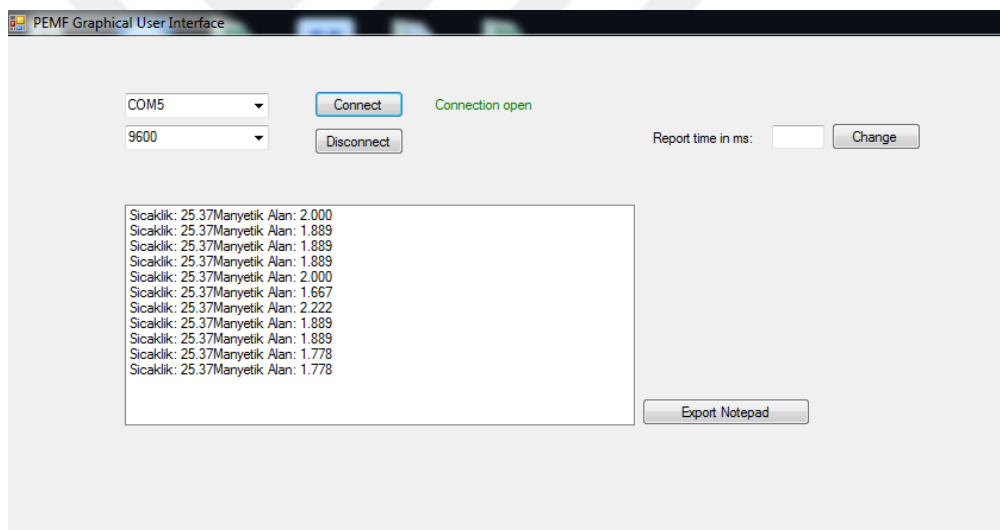


Figure 5.11 : Interface program save sensor datas during the experiment.

5.7 Comparison of the Sensor Network Measurement and Simulation Results

We have made comparisons, Arduino based sensor data that we use is in accordance with the actual values. While the sensors connected to an Arduino are in the transmitter position in the system, the other Arduino embedded LattePanda is the receiver of the system.

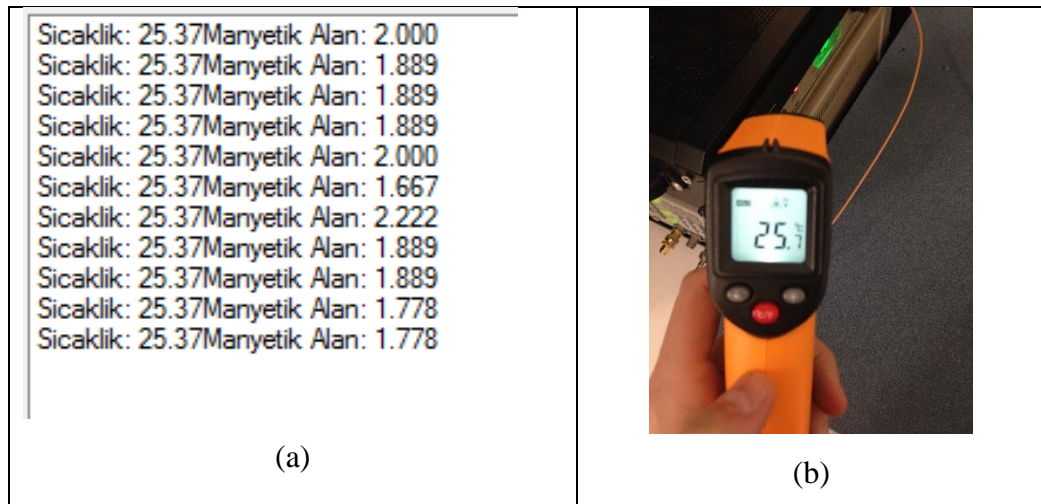


Figure 5.12 : (a)Received temperature value is 25.37 °C with DS18B20 sensor (b) and 25.7 °C on petri dish with the infrared sensor.

When the system sensor DS18B20 temperature in the immediate vicinity of the petri dish is 25.37 °C, we measure 25.7 °C on petri dish with the infrared sensor (Figure 5.12).

6. PERFORMANCE OF THE PEMF AND PRFE SYSTEMS IN VITRO EXPERIMENT

6.1 Overview

We support the prototypes we produce for in-depth knowledge of our studies with in vitro experiments. For this purpose, we grouped all experimental groups as PEMF 1, PEMF 2 and PRFE and examined the magnetic field changes in L929 cell line. The experiment was 4 hours exposing all cell lines simultaneously, exposing the magnetic field to the same environment. Wounds on the cell lines were taken at regular intervals. Microscope screens were taken by inverted microscope after exposure in initial time (zero), 12th, 24th, 36th, 48th, 60th and 72th hours. After the wound closure percentages were calculated and significant results were found.

6.1.1 Material and Methods

L929 fibroblast cell line is taken by Izmir Katip Çelebi University Department of Biomedical Engineering. Cells were growth in Dulbecco's Modified Eagle Medium (DMEM) which includes 0.1% penicillin/streptomycin (Sigma-Aldrich, Steinheim), 10% FBS (Sigma-Aldrich, Steinheim), 1% L-glutamine (Gibco, Grand Island, US), and incubated at 37° C and 5% CO₂. 5x10⁴ cells seeded into 24 well plates. After incubation time in overnight, wound model was realized on cells by using 200 µl pipette tips. After all well washed with Phosphate Buffer Saline (PBS), fresh media was added into well plate. Wound model was constructed for PEMF1, PEMF2 and PRFE exposure systems. Every experiment was done 3 times (n=3).

6.2 PEMF and PRFE Exposure System

Three different exposure systems were applied into wound model. They are PEMF1, PEMF2 and PRFE. Healing range of each group is compared with control group which

is non treatment. Each exposure system was performed during 4 hours. Microscope screens were taken by inverted microscope after exposure in initial time (zero), 12th, 24th, 36th, 48th, 60th and 72th hours (Olympus CKX41-Tokio, Japan). Wound closing percentage range was evaluated by ImageJ (NIH) software in zero and 72th hours.

6.2.1 Simulations and Biological Results of PEMF and PRFE

Exposure to L929 Cells

Wound healing process was given for control, PEMF1, PEMF2 and PRFE groups at different times. Experimental groups were compared with the control group for each time point (Figure 6.1). As soon as exposure during 4 hours, images were taken and they have shown that wound closing ratio is nearly the same for every group. Actually, PEMF1 has less gap than control and others. Figures have demonstrated that starting of the wound healing process was after 12th hours. Especially, PEMF1 group cells started to cover well surface and other exposure groups have started to wound healing process. In the end of 24th hours, PRFE groups have belonged better healing compared with control and other experimental groups in same time point. PRFE group has exhibited that wound model closed nearly 90% ratio in 36th hours while other experimental groups closed the well. Moreover, end of 48th hours, PEMF healed completely all surface and PRFE2 nearly closed, too. While PRFE2 exposure system was nearly completed in end of 60th hours, control group has not closed implicitly.

After exposure time, microscope images of each group exposure were taken immediately. Wound healing time and percentage values of PEMF 1, PEMF2 and PRFE systems were given in Fig 6.1 zero and after 72 th hours. Average ratios were measured $17,24 \pm 6,25\%$ for control group, $27,43 \pm 2,11\%$ for PEMF1 ($p^* < 0,05$), $23,03 \pm 5,95\%$ $22,06 \pm 5,14\%$ for PRFE after treatment. However, they were measured $87,07 \pm 4,34$, $97,05 \pm 2,84$ ($p^* < 0,01$), $95,67 \pm 5,90$ ($p^* < 0,05$), $98,24 \pm 1,83$ ($p^{**} < 0,01$) in 72th hours, respectively.

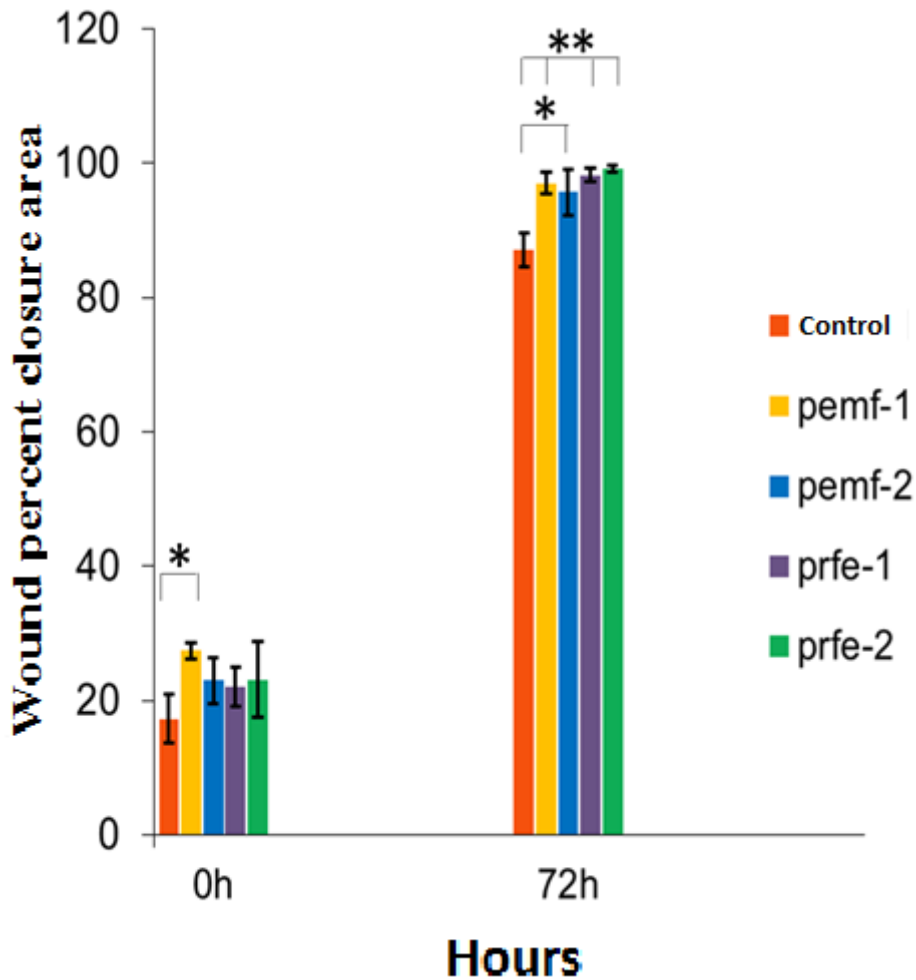


Figure 6.1: Wound percent closure area comparison chart.

All results have presented that PEMF1 is effective after treatment in zero and PEMF2 and PRFE groups are also efficient on L929 wound healing process relatively control group. Therefore, L929 fibroblast cell line covered well surface and provided to heal. In different time point, cell numbers have been increased by the exposure system but PRFE has captured a trend in increasing cell number. The reason for this, it is influential in long term exposure. As previous studies in the literature are pointed out that PEMF and PRFE systems contribute to enhance the wound healing process at 72th hours.

End of experiment three exposed groups compared to the control group, wounds in L929 cell lines hadn't closed yet. All group was closed in 72nd hours although the control group was not (Figure: 6.2).

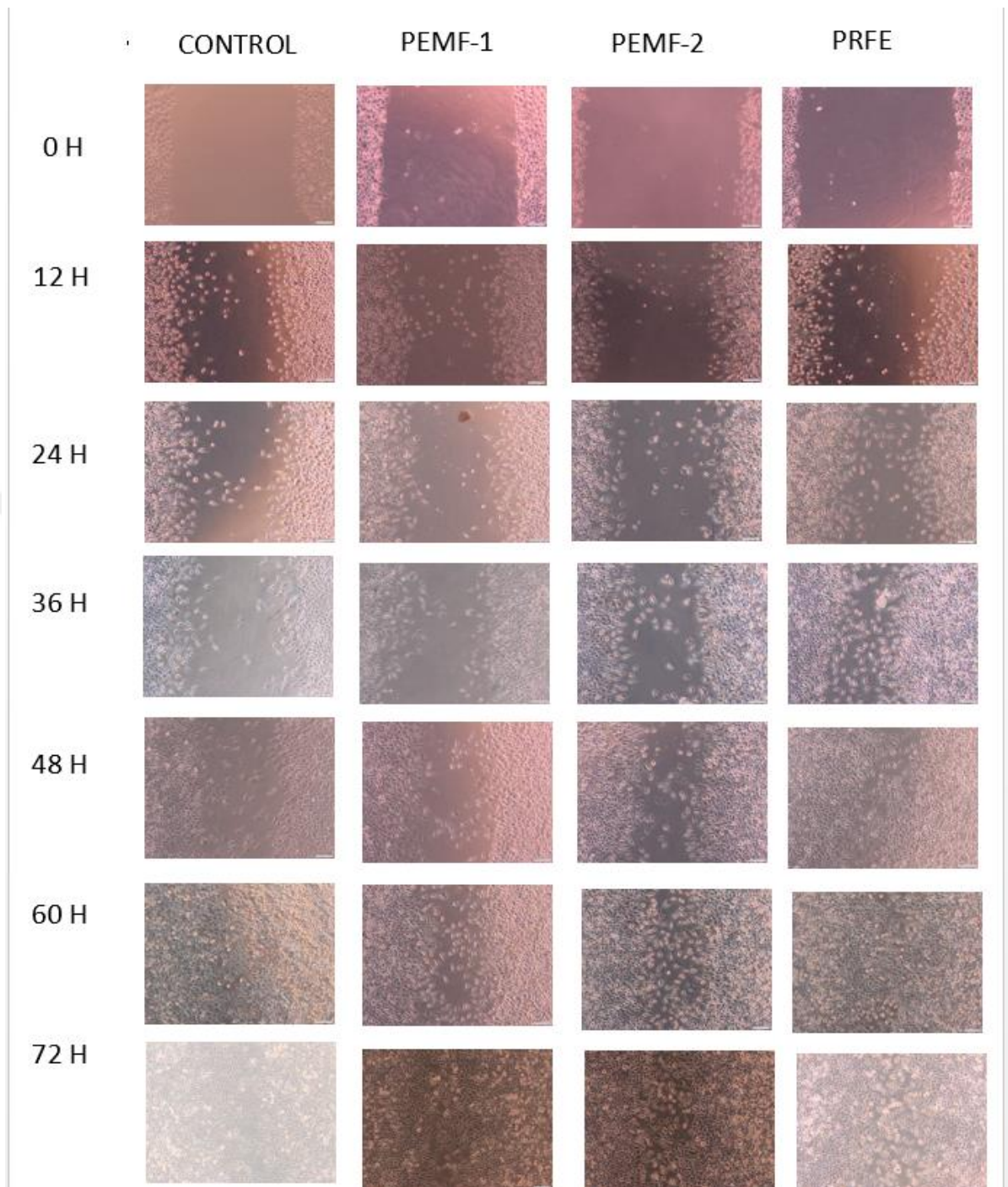


Figure 6.2. : Microscopic images of PEMF-exposed, PRFE-exposed and control group L929 cell line.

This study has estimated that different PEMF and PRFE treatment supported to heal process as previous studies in bone tissue engineering and wound healing. While efficiency of 75 Hz frequency PEMF is not known on cellular responses, PEMF affects wound healing owing to synthesis of DNA, protein and growth factor and nitric acid

production. Seeliger and friends proved that PEMF application enhanced cell proliferation and migration [34]. At the same time, PRFE increased cellular response on wound model. Moffett asserted proliferative effect of PRFE on fibroblast and keratiocyte cell in mRNA level [35]. This study has shown that both PEMF and PRFE applications affect cell proliferation and migration, as well as the comparison of the categories within these groups. It was observed that all experimental group results are better than control group in the end of 72th day.



7. CONCLUSION

In this study, the EMF system has been developed to investigate the effects of pulsed electromagnetic fields on treatment and as a result, using this system and accelerate tissue healing was achieved. In addition to many studies conducted in the literature in different forms, a sensor network supported this study. With the designed coil and Helmholtz coil, the low frequency PEMF system experiments at 75 Hz and simulations were successfully completed. The result of the experiment showed that the L929 fibroblast cell line exposed to the electromagnetic field closes the wound faster than the control group. The data obtained during the experiment showed that the temperature change was negligible for PEMF and PRFE systems known as nonthermal. Wireless sensor network was installed with XBee, LattePanda, Arduino, DS18B20 temperature sensor, MLX90614 infrared temperature sensor and DRV5053 magnetic field sensor. In this system, temperature and magnetic field changes were recorded by WSN for environmental monitoring with LattePanda during the experiment. The basis of wireless communication XBee network configuration, used at router and coordinator mode. Data transmission implemented were used in AT mode to accommodate sensor node packet receiver (RX) and transmitter (TX).

I present the main results of this study that we investigated the effects of pulsed electromagnetic field with the help of wireless sensor network:

- In the electromagnetic field wound healing studies, it has been shown that the magnetic field applied during the test assisted by the wire sensor network can be measured successfully and whether there is a temperature change in the exposed area.
- With the antenna used at 27 MHz, PRFE system was used to obtain the best wound healing among all experimental setups. The impedance matching for this antenna has been shown to be better than the results obtained by adaptation.

- It has been shown that it can be developed flexibly and developed in the Kapton antenna and can be used in accordance with PRFE experiments.
- In the experiment, we called PEMF 1 with the designed coil with a 4 mT electromagnetic field exposed to the wound in the cell line, PEMF 2 we called the Pasco Helmholtz coil with 1 mT electromagnetic field in the cell line we concluded that the wound was better than wound healing.
- We have shown that the wireless sensor network helps control the system in 4 hours of experiments. We have observed the changes in the magnetic field that we applied during the experiment and recorded the data.

The effect of the mechanisms we use in different tissues and animal experiments should be investigated. Our findings contribute to the development of subjects such as wound healing, tissue regeneration and cancer tissues. When the mechanisms used by the PEMF system are understood, it is thought to provide a more effective treatment in future studies. Once these studies are completed, the contribution of EMF applications to treatments will be much greater.

REFERENCES

1. Becker, R. O. (2004). Exploring new horizons in electromedicine. *The Journal of Alternative and Complementary Medicine*, 10(1), 17–18.
doi:10.1089/107555304322848904.
2. Malmivuo, J. & R. Plonsey. (1995). *Bioelectromagnetism: Principles and Applications of Bioelectric and Biomagnetic Fields*. Oxford University Press: USA.
3. Guy, A.W. (1984). History of biological effects and medical applications of microwave energy. *IEEE Transactions on Microwave Theory and Techniques*. 32(9), 1182-1200.
4. Maxwell, J.C. (1865). VIII. A Dynamical theory of the electromagnetic field. *Philosophical Transactions of The Royal Society of London*, 155, 459-512.
5. Aaron, R.K. & D.M. Ciombor (1993). Therapeutic effects of electromagnetic fields in the stimulation of connective tissue repair. *Journal of Cellular Biochemistry*, 52(1), 42-46.
6. Brust, M., et al. (1994). Synthesis of thiol-derivatised gold nanoparticles in a two-phase liquid–liquid system. *Journal of the Chemical Society, Chemical Communications*, (7), 801-802.
7. Tao, Q. & A. Henderson. (1999). EMF induces differentiation in HL-60 cells. *Journal of Cellular Biochemistry*. 73(2), 212-217.
8. Tofani, S., et al. (2002). Increased mouse survival, tumor growth inhibition and decreased immunoreactive p53 after exposure to magnetic fields. *Bioelectromagnetics*, 23(3), 230-238.
9. Pappas, P. (1971-1996), (1983). The original Ampere force and Biot-Savart and Lorentz forces. *Il Nuovo Cimento B*, 76(2), 189-197.
10. Restrepo-Alvarez, A.F., E. Franco-Mejia, & C.R. Pinedo-Jaramillo. (2012). *Study and Analysis of Magnetic Field Homogeneity of Square and Circular Helmholtz Coil Pairs: A Taylor Series Approximation*. VI Andean Region International Conference Andescon, Cuenca, Ecuador.
11. Staebell, K.F. & D. Misra. (1990). An experimental technique for in vivo permittivity measurement of materials at microwave frequencies. *IEEE Transactions on Microwave Theory and Techniques*, 38(3), 337-339.
12. Augustine, R. (2009). *Electromagnetic Modelling of Human Tissues and Its Application on The Interaction Between Antenna and Human Body in The BAN Context*, Université Paris-Est, Paris.
13. Da Graça Lopes, C.A. (2010). *Characterisation of The Radio Channel in On-Body Communications*. Ph. D. Thesis. Universidade Técnica de Lisboa, Lisboa, Portugal.
14. Teo, M., et al. (2008). Development of magneto-dielectric materials based on Li-ferrite ceramics: II. DC resistivity and complex relative permittivity. *Journal of Alloys and Compounds*, 459(1-2): p. 567-575.

- 15.Kumar, S. & A. Kaur. (2010). Shadow detection and removal in color images using Matlab. *International Journal of Engineering Science and Technology*, 2(9): p. 4482-4486.
- 16.Longo, F., et al. (1999). Electromagnetic fields influence NGF activity and levels following sciatic nerve transection. *Journal of Neuroscience Research*, 55(2): p. 230-237.
- 17.Goodman, R. & M. Blank. (2002). Insights into electromagnetic interaction mechanisms, *Journal of Cellular Physiology*, 192(1),16-22.
- 18.Islamov, R.R., et al. (2002). 17 β -estradiol stimulates regeneration of sciatic nerve in female mice, *Brain Research*, 943(2), 283-286.
- 19.Fitzsimmons, R.J., et al. (2008). A pulsing electric field (PEF) increases human chondrocyte proliferation through a transduction pathway involving nitric oxide signaling. *Journal of Orthopaedic Research*, 26(6), 854-859.
- 20.Bassett, C. (1989). Fundamental and practical aspects of therapeutic uses of pulsed electromagnetic fields (PEMFs). *Crit Rev Biomed Eng*, 17(5), 451-529.
- 21.Rubik, B. (1997). Bioelectromagnetics & the future of medicine. *Administrative Radiology Journal*, 16(8): p. 38-46.
- 22.Stiller, M., et al. (1992). A portable pulsed electromagnetic field (PEMF) device to enhance healing of recalcitrant venous ulcers: a double-blind, placebo-controlled clinical trial. *British Journal of Dermatology*, 127(2): p. 147-154.
- 23.Omote, Y., et al. (1990). Treatment of experimental tumors with a combination of a pulsing magnetic field and an antitumor drug. *Japanese Journal of Cancer Research*, 81(9): p. 956-961.
- 24.Ieran, M., et al. (1990). Effect of low frequency pulsing electromagnetic fields on skin ulcers of venous origin in humans: A double-blind study. *Journal of Orthopaedic Research*, 8(2): p. 276-282.
- 25.Scaiano, J., F.L. Cozens, & J. McLean. (1994). Model for the rationalization of magnetic field effects in vivo. Application of the radical-pair mechanism to biological systems. *Photochemistry and Photobiology*, 59(6): p. 585-589.
- 26.Lander, H.M. (1997). An essential role for free radicals and derived species in signal transduction. *The FASEB Journal*, 11(2): p. 118-124.
- 27.Lin, J.C. (2003). Safety standards for human exposure to radio frequency radiation and their biological rationale. *IEEE Microwave Magazine*, 4(4): p. 22-26.
- 28.Zborowski, M., et al. (2003). Magnetic field visualization in applications to pulsed electromagnetic field stimulation of tissues. *Annals of Biomedical Engineering*, 31(2): p. 195-206.
- 29.Firester, A.H. (1966). Design of square Helmholtz Coil system. *Review of Scientific Instruments*, 37(9): p. 1264-1265.
- 30.Banzi, M. & M. Shiloh. (2014). *Getting Started With Arduino: The Open Source Electronics Prototyping Platform*. United State of America: Maker Media, Inc.
- 31.Faludi, R. (2010). *Building Wireless Sensor Networks: With Zigbee, Xbee, Arduino, And Processing*. United State of America: O'Reilly Media, Inc.
- 32.<https://www.electronics-tutorials.ws/electromagnetism/hall-effect.html>
- 33.Xu, Y., et al. (2017). A Switching Arc Plasma Measurement Experimental System Using A Magnetic Sensor Array. 2017 4th International Conference on, IEEE, China.

34. Takahashi, K., et al. (1986). Effect of pulsing electromagnetic fields on DNA synthesis in mammalian cells in culture. *Experientia*, 42(2): p. 185-186.
35. Lee, G., et al. (2016). A reconfigurable resonant coil for range adaptation wireless power transfer. *IEEE Transactions on Microwave Theory and Techniques*, 64(2): p. 624-632
36. Technical Committee 95 (2014), Draft standard for military workplaces -force health protection regarding personnel exposure to electric, magnetic and electromagnetic fields, 0 Hz to 300 GHz. *IEEE International Committee on Electromagnetic Safety*.



CURRICULUM VITAE

Name Surname: Merve Bardak

Date of Birth: 07/05/1990

E-Mail: m.bardak1@gmail.com

M.Sc.: Izmir Katip Celebi University, Department of Biomedical Technologies, 2019

B.Sc.: Atilim University-Engineering Faculty Department of Electric and Electronic Engineering, 2013

PUBLICATIONS, PRESENTATIONS AND PATENTS ON THE THESIS:

- **M. Bardak, Z. B. Yaralı, A. Kaya, O. Karaman,**” Research on The Effect of Wound Healing on Pulsed Electromagnetic Field and Pulsed Radiofrequency Applications With Sensor Technologies”, *1st International Health Sciences and Life Congress*, Burdur, 02-05 May 2018
- **M. Bardak, A. Kaya,** “Darbeli Elektro Manyatik Alanların Üretilmesi ve Kontrollü Alanların Sıçan Derisinde Oluşturulan Yaraya Etkisi” 2. Uluslararası Lisansüstü Eğitim Kongresi, Manisa, 12-14 Mayıs 2017

COMPUTER SKILLS AND COMPETENCES

CST Studio, Android Studio, Proteus, MATLAB, Arduino, Microsoft Office